Electronic Supplementary Information

Bis(*N*-acylated imidazolin-2-imine) Nickel Catalyzed Norbornene Copolymerization with Methyl Acrylate

Yanqing Li [a, b], Hu Zhang [a], Ru Xiao [a]* and Zhengguo Cai [a] *

[a] State Key Laboratory for Modification of Chemical Fibers and Polymer Materials, College of Materials Science and Engineering, Donghua University, Shanghai 201620, P. R. China

[b] College of Biological and Chemical Engineering, Guangxi University of Science and Technology, Liuzhou 545006, P. R. China

Contents

1. Synthetic Procedure

1.1 Synthesis of *N*-acylated imidazolin-2-imine ligands (L1-L4) and NMR spectra of compounds

Scheme S1. Synthesis of Mono-substituted *N*-acylated imidazolin-2-imine Ligands (**L1-L2**)

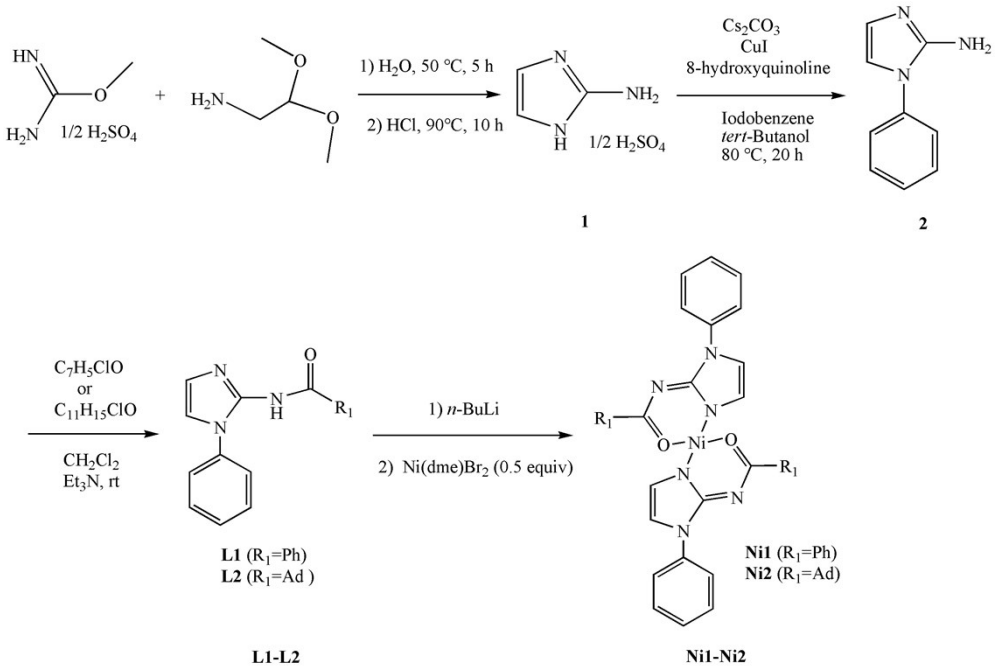

Scheme S2. Synthesis of Bis-substituted *N*-acylated imidazolin-2-imine Ligands (**L3-L4**)

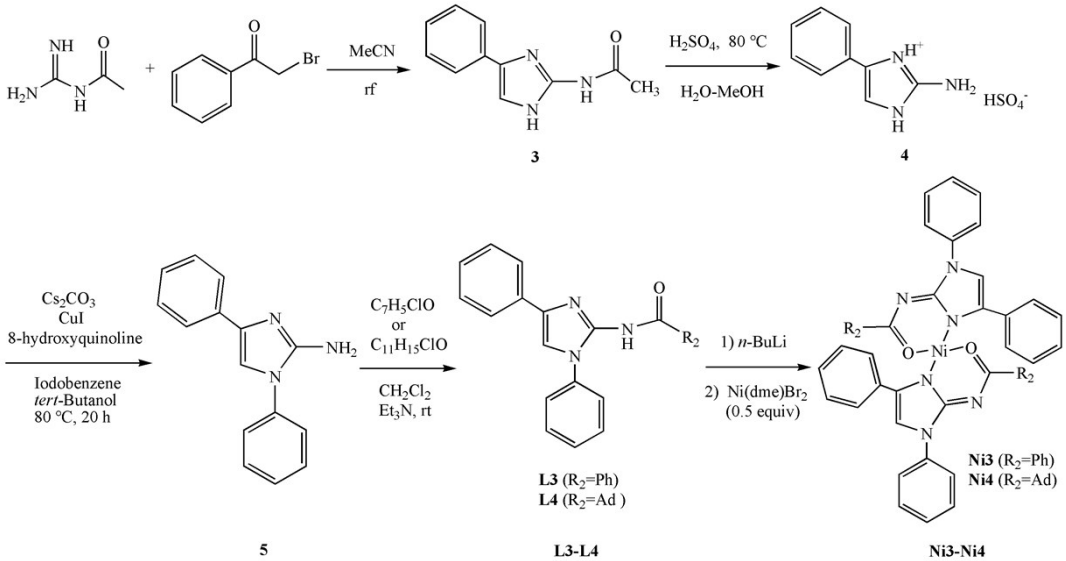

Synthesis of 2-amino-1*H*-imidazole hemisulfate (1): A 250 mL two-neck flask was charged with 2-aminoacetaldehyde dimethyl acetal (5.56 mL, 50 mmol), O-methylisourea hemisulfate (6.25 g, 50 mmol) and 30 mL water, and stirred for 1 h at room temperature. The temperature was then elevated up to 50 °C and kept for 5 h. Subsequently, the 10 mL of concentrated hydrochloric acid was introduced, and the mixture was heated to 90 °C for another 10 h. The solvent was evaporated, and the solid was dissolved in a mixed solution of ethanol and water (volume ratio, 1:1) and crystallized under minus 20 degrees Celsius to get a white crystal (4.95 g, 37.46 mmol, 74.92%). ^{1}H NMR (D_2O, δ, ppm): 6.73 (s, 2H, =CH). ^{13}C NMR (D_2O, δ, ppm): 146.55, 112.83.

Synthesis of 1-phenyl-1*H*-imidazol-2-amine (2): 2-Amino-1*H*-imidazole hemisulfate (5.29 g, 40 mmol) was dissolved in H_2O and neutralized with 1 mol/L NaOH, and dried under vacuum. The precipitate was collected and mixtured with Cs_2CO_3 (19.75 g, 60 mmol), CuI (0.78 g, 4 mmol) and 8-hydroxyquinoline (0.89 g, 6 mmol), and anhydrous *t*-BuOH (80 mL), and iodobenzene (4.55 mL, 40 mmol) were injected in turn into the mixture solution. The solution was heated up to 80 ℃ and maintained with stirring. After 20 h, the solvent was removed under vacuum, and the product was extracted using EtOAc (3×50 mL) and the organic layer was filtered through a 0.45 μm millipore membrane filter. The EtOAc was evaporated in vacuo, the crude products were purified by recrystallization in a mixture of toluene and hexane (4.58 g, 28.81 mmol, 72.02%). ^{1}H NMR (DMSO, δ, ppm): 7.46-7.50 (m, 5H, =CH, -NH), 7.36 (t, 1H, =CH), 6.93 (s, 1H, =CH), 6.63 (s, 1H, =CH), 5.46 (s, 2H, -

NH_2). ^{13}C NMR (DMSO, δ, ppm): 149.57, 138.05, 130.03, 127.17, 125.37, 124.38, 116.32.

Synthesis of 2-acetamido-4-phenyl-1*H*-imidazole (3). A 250 mL oven-dried flask was charged with 2-bromoacetophenone (4.02 g, 20 mmol) and 1-acetylguanidine (6.19 g, 60 mmol) in 40 mL acetonitrile, and the solution was then refluxed at 85 ℃ for 19 h. As the reaction was complete, the solvent was removed under vacuum. Purification of the resulting material by recrystallization in a mixture of THF and hexane afforded a white solid (1.35 g, 6.71 mmol, 33.55%). ^1H NMR (DMSO, δ, ppm): 11.64 (s, 1H, -NH), 11.28 (s, 1H, -NH), 7.64 (d, 2H, =CH), 7.54 (bs, 2H, $-NH_2$), 7.45 (t, 2H, =CH), 7.43 (s, 1H, =CH), 7.34 (t, 1H, =CH). ^{13}C NMR (DMSO, δ, ppm): 148.24, 129.42, 128.42, 128.18, 126.89, 124.50, 110.02.

Synthesis of 2-amino-4-phenyl-1*H*-imidazole sulfate (4). 2-Acetamido-4-phenyl-1*H*-imidazole (2.01 g, 10 mmol) was dissolved in a mixture solution of methanol and water (60 mL, volume ratio=1:1), and 0.60 mL of concentrated sulfuric acid was added. The mixture solution was subsequently heated and stirred at 100 °C for 16 h. After cooling to 0 °C℃, the colorless crystal was obtained at high yield (2.47 g, 9.60 mmol, 96.01%). ^1H NMR (DMSO, δ, ppm): 12.68 (s, 1H, -NH), 12.06 (s, 1H, -NH), 7.64 (D, 2H, =CH), 7.32 (t, 2H, =CH), 7.26 (s, 1H, =CH), 7.16 (t, 1H, =CH), 2.07 (s, 3H, $-CH_3$). ^{13}C NMR (DMSO, δ, ppm): 169.01, 141.72, 136.54, 135.14, 128.87, 126.34, 124.40, 109.67, 23.28.

Synthesis of 1,4-diphenyl-1*H*-imidazol-2-amine (5). 1,4-Diphenyl-1*H*-imidazol-2-amine was synthesized in a similar method producing 1-phenyl-1*H*-imidazol-2-amine.

The general procedure using 2-amino-4-phenyl-1*H*-imidazole sulfate (2.57, 10 mmol) provided a white solid that crystallized from CH_2Cl_2 to yield a colorless crystal (1.28 g, 5.44 mmol, 54.40%). ^{1}H NMR ($CDCl_3$, δ, ppm): 7.74 (d, 2H, =CH), 7.54 (t, 2H, =CH), 7.48 (d, 2H, =CH), 7.43 (t, 1H, =CH), 7.38 (t, 2H, =CH), 7.24 (t, 2H, =CH), 7.06 (bs, 2H, -NH_2). ^{13}C NMR ($CDCl_3$, δ, ppm): 147.55, 137.73, 136.89, 133.93, 129.98, 128.55, 127.97, 126.56, 124.65, 124.43, 111.47.

Synthesis of *N*-(1-phenyl-1*H*-imidazol-2-yl)benzamide ligand (L1). 1-Phenyl-1*H*-imidazol-2-amine (1.59 g, 10 mmol) was dissolved in dichloromethane (60 mL) in a 250 mL flask and triethylamine (1.50 mL, 11 mmol) was added, and then benzoyl chloride (1.16 mL, 10 mmol) was injected with a syringe. After stirring for 10 h at 25 ℃, the mixture solution was removed under vacuum. The crude product was purified by silica gel column chromatography (eluent: EtOAC/Hexane=1:3) to give **L1** (2.03 g, 77%). ^{1}H NMR ($CDCl_3$, δ, ppm): 12.61 (brs, 1H, -NH), 8.22 (d, 2H, =CH), 7.71 (d, 2H, =CH), 7.54 (t, 2H, =CH), 7.46 (t, 1H, =CH), 7.40 (q, 4H, =CH), 6.88 (d, 2H, =CH). ^{13}C NMR ($CDCl_3$, δ, ppm): 174.57, 149.75, 137.85, 136.60, 130.90, 129.18, 128.87, 127.92, 127.61, 124.59, 114.87, 113.16.

Synthesis of *N*-(1-phenyl-1*H*-imidazol-2-yl) adamantanecarboxamide ligand (L2). **L2** was synthesized in a similar way to that for **L1** in 71% yield. ^{1}H NMR (DMSO, δ, ppm): 9.44 (s, 1H, -NH), 7.48 (t, 2H, =CH), 7.36-7.40 (m, 4H, =CH), 6.99 (s, 1H, =CH), 1.94 (s, 3H, -CH_2), 1.70 (s, 6H, -CH) , 1.65 (q, 6H, -CH_2). ^{13}C NMR (DMSO, δ, ppm): 178.06, 138.44, 137.23, 129.53, 128.08, 126.85, 124.75, 121.00, 40.67, 38.70, 36.43, 27.96.

Synthesis of *N*-(1,4-diphenyl-1*H*-imidazol-2-yl)benzamide ligand (L3). L3 was synthesized in a similar way to that for **L1** in 63% yield. ^{1}H NMR ($CDCl_3$, δ, ppm): 7.83 (d, 2H, =CH), 7.67 (d, 4H, =CH), 7.47 (t, 2H, =CH), 7.42 (t, 2H, =CH), 7.39 (t, 2H, =CH), 7.34 (s, 1H, -NH), 7.33 (d, 2H, =CH), 7.19 (d, 2H, =CH). ^{13}C NMR (DMSO, δ, ppm): 171.95, 141.13, 138.95, 135.55, 133.58, 133.46, 132.80, 129.60, 129.29, 128.91, 128.61, 128.40, 127.31, 125.08, 125.02, 116.23.

Synthesis of *N*-(1,4-diphenyl-1*H*-imidazol-2-yl)adamantanecarboxamide ligand (L4). L4 was synthesized in a similar way to that for **L1** in 66% yield. ^{1}H NMR ($CDCl_3$, δ, ppm): 11.04 (b, 1H, -NH), 7.90 (s, 2H, =CH), 7.49 (t, 1H, =CH), 7.42 (t, 2H, =CH), 7.33 (s, 3H, =CH), 6.78 (s, 2H, =CH), 1.97 (s, 3H, -CH), 1.77 (s, 6H, $-CH_2$) , 1.68 (q, 6H, $-CH_2$). ^{13}C NMR (DMSO, δ, ppm): 169.85, 158.54, 130.73, 130.53, 129.77, 129.72, 128.51, 128.39, 127.18, 126.76, 102.17, 99.37, 43.94, 38.90, 36.69, 28.17.

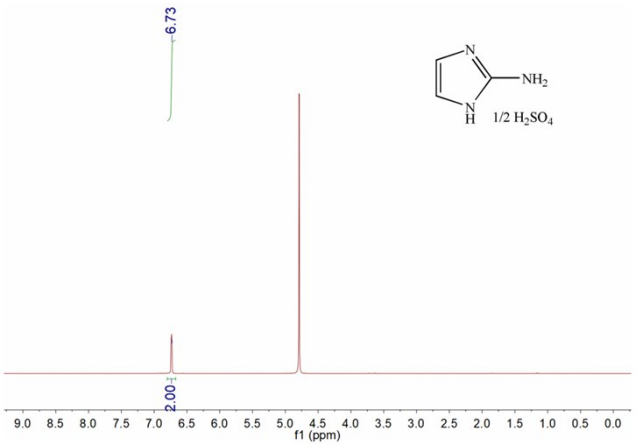

Figure S1-1. ^{1}H NMR spectrum of compound **1** in D_2O

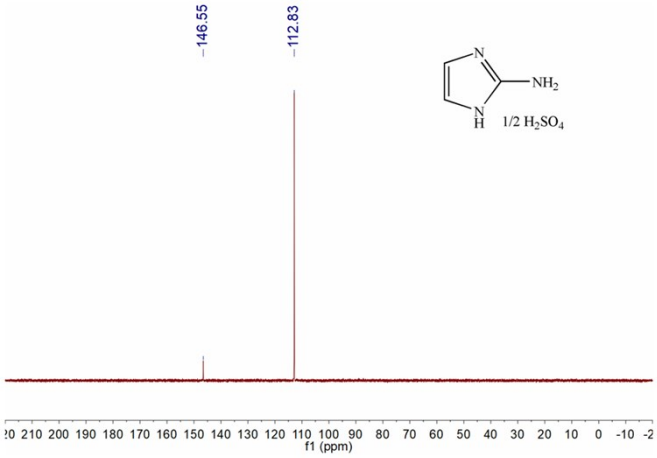

Figure S1-2. ^{13}C NMR spectrum of compound **1** in D_2O

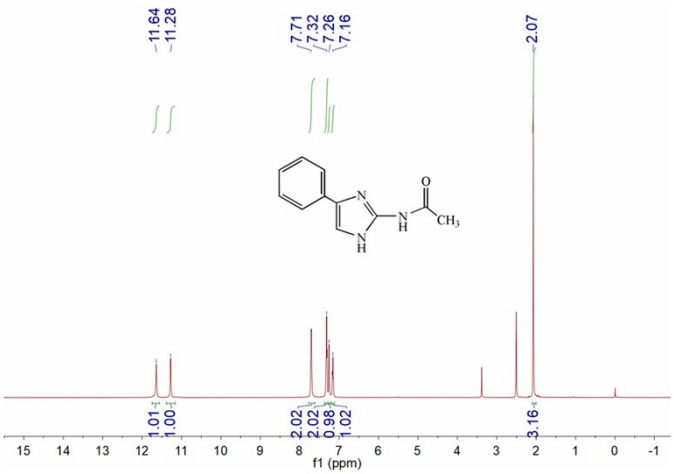

Figure S1-3. ^{1}H NMR spectrum of compound **2** in DMSO

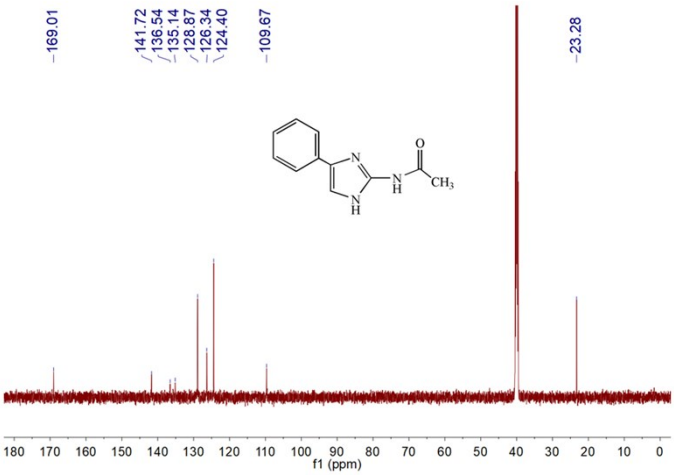

Figure S1-4. ^{13}C NMR spectrum of compound **2** in DMSO

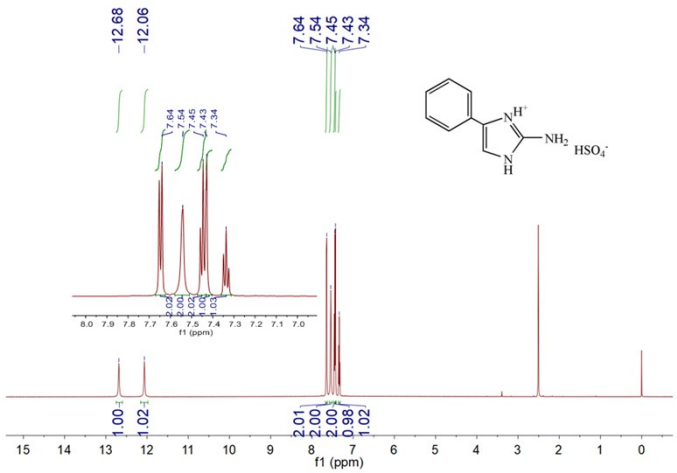

Figure S1-5. ^{1}H NMR spectrum of compound **3** in DMSO

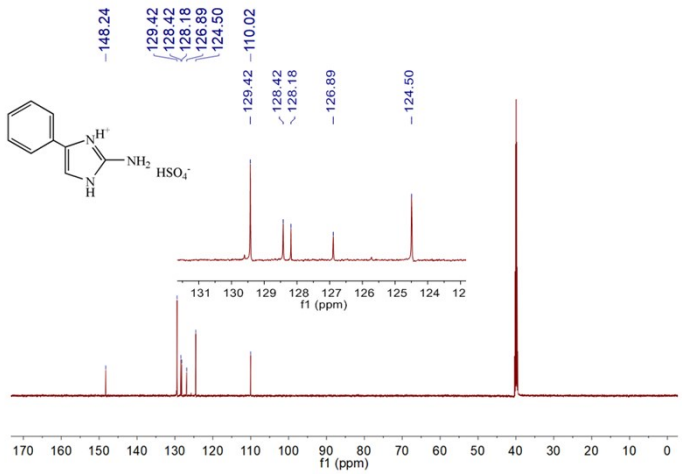

Figure S1-6. ^{13}C NMR spectrum of compound **3** in DMSO

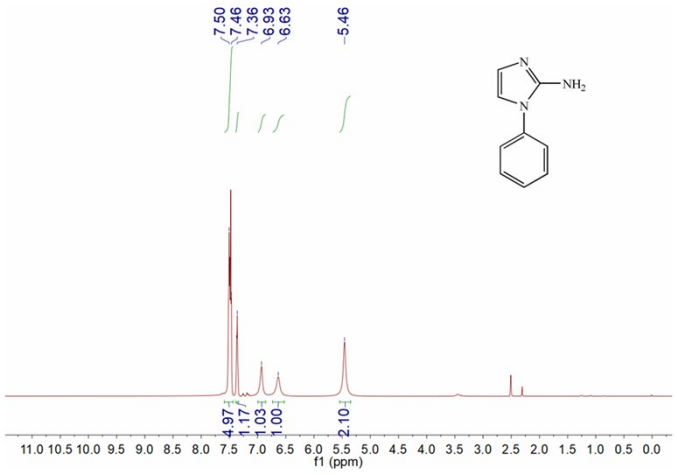

Figure S1-7. ^{1}H NMR spectrum of compound **4a** in DMSO

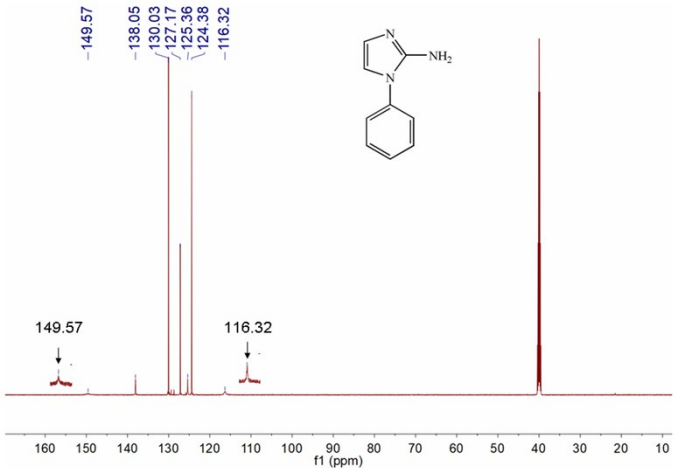

Figure S1-8. ^{13}C NMR spectrum of compound **4a** in DMSO

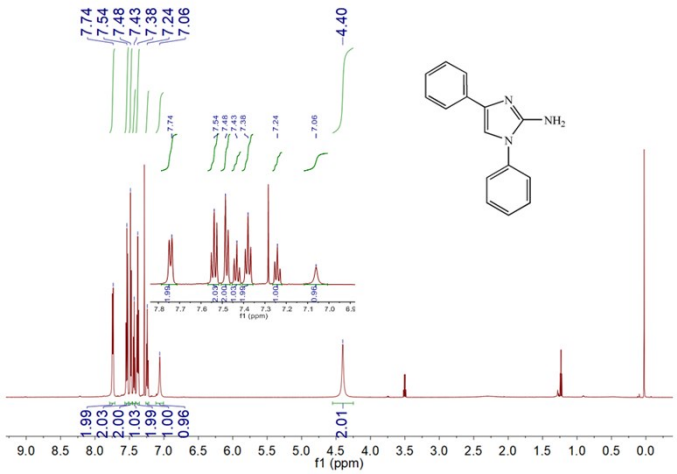

Figure S1-9. ^{1}H NMR spectrum of compound **4b** in $CDCl_3$

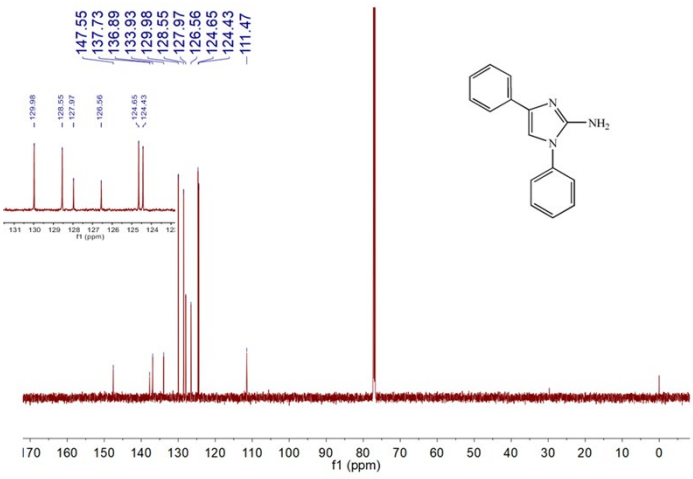

Figure S1-10. ^{13}C NMR spectrum of compound **4b** in $CDCl_3$

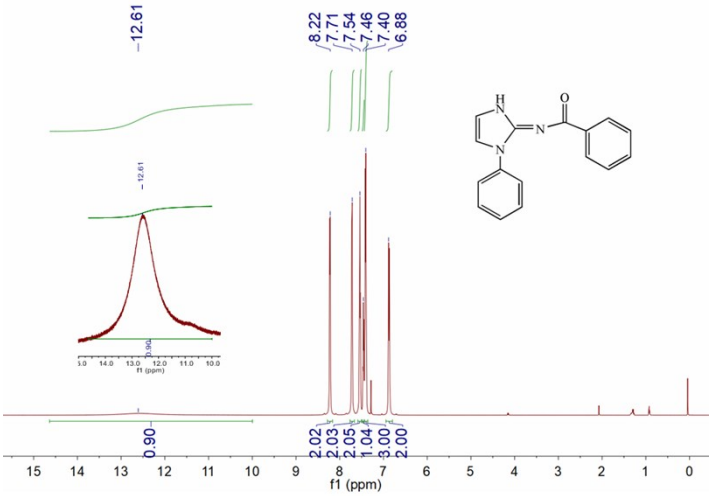

Figure S1-11. ^{1}H NMR spectrum of compound **L1** in $CDCl_3$

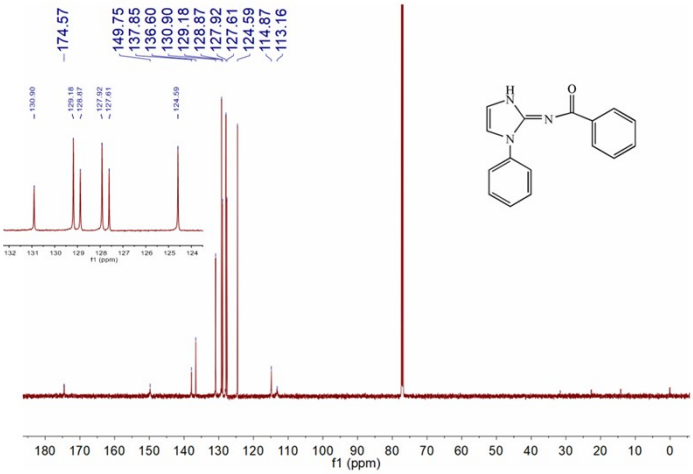

Figure S1-12. ^{13}C NMR spectrum of compound **L1** in $CDCl_3$

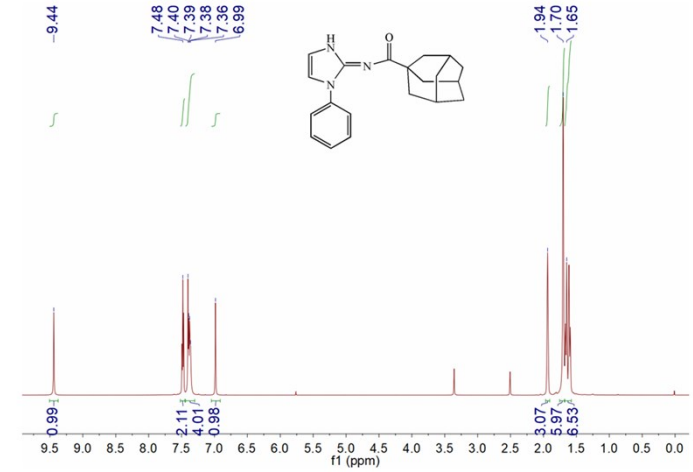

Figure S1-13. ^{1}H NMR spectrum of compound **L2** in $CDCl_3$

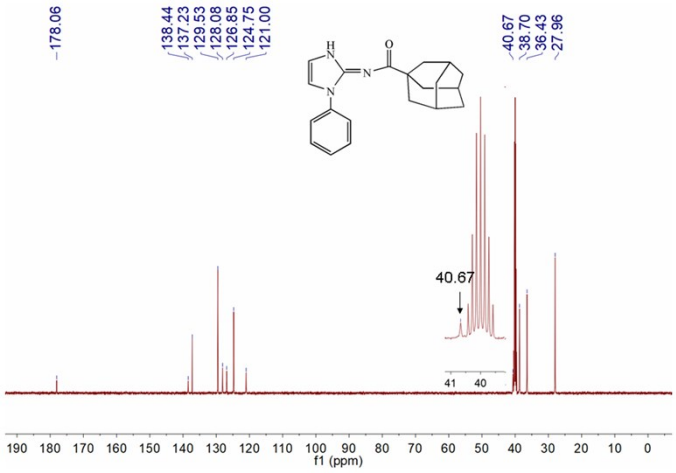

Figure S1-14. ^{13}C NMR spectrum of compound **L2** in $CDCl_3$

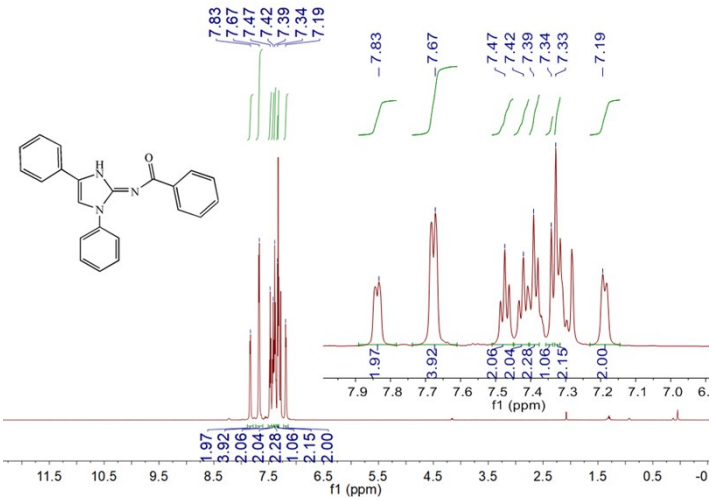

Figure S1-15. ^{1}H NMR spectrum of compound **L3** in $CDCl_3$

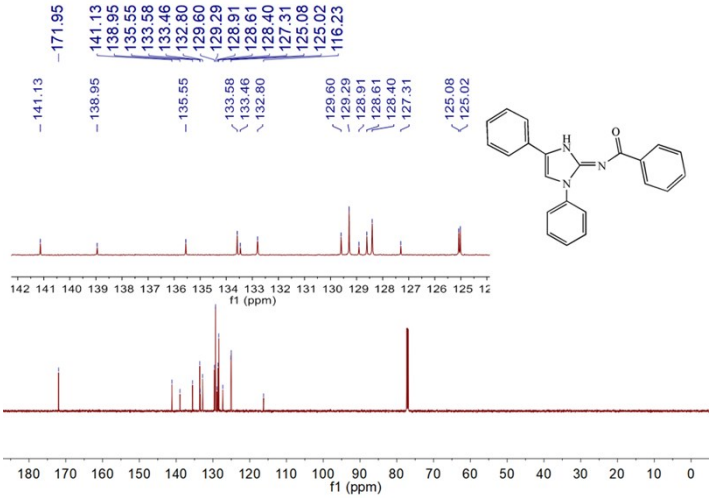

Figure S1-16. ^{13}C NMR spectrum of compound **L3** in $CDCl_3$

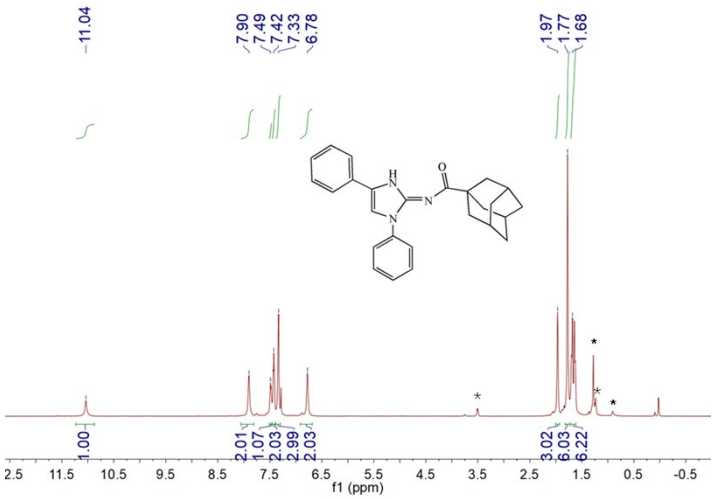

Figure S1-17. ^{1}H NMR spectrum of compound **L4** in $CDCl_3$ (* - H grease; ⁎ - diethyl ether)

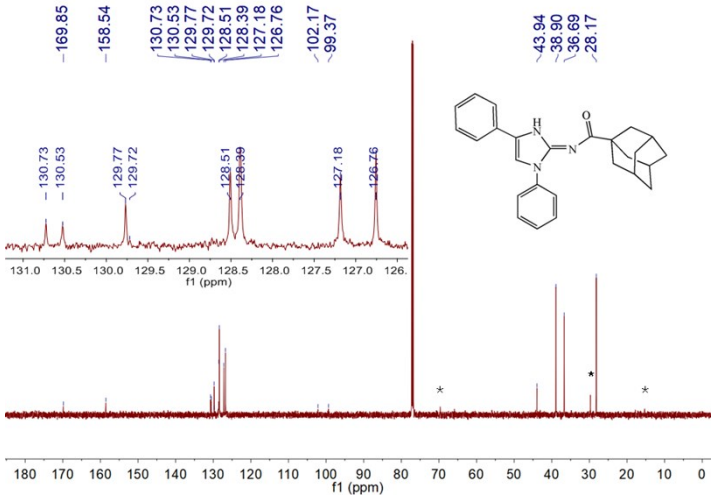

Figure S1-18. ^{13}C NMR spectrum of compound **L4** in $CDCl_3$ (* - H grease; ⁎ - diethyl ether)

1.2 ^{1}H NMR spectra of nickel complexes

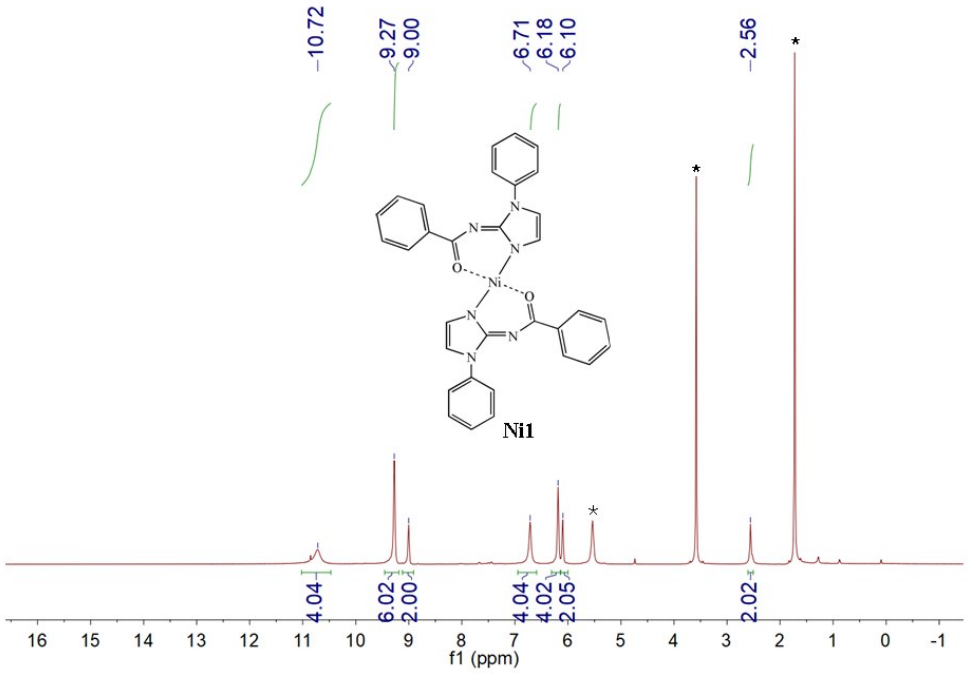

Figure S1-19. ^{1}H NMR spectrum of complex **Ni1** in THF-d_8 (* - THF-d_8; ⁎ - CH_2Cl_2)

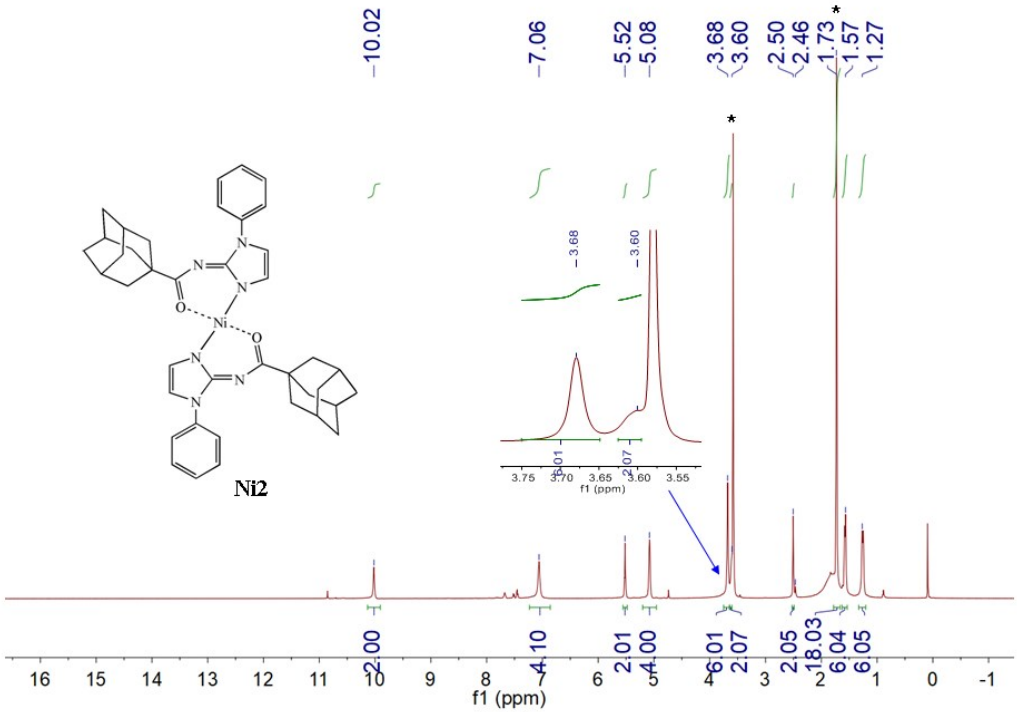

Figure S1-20. ^{1}H NMR spectrum of complex **Ni2** in THF-d_8 (* - THF-d_8)

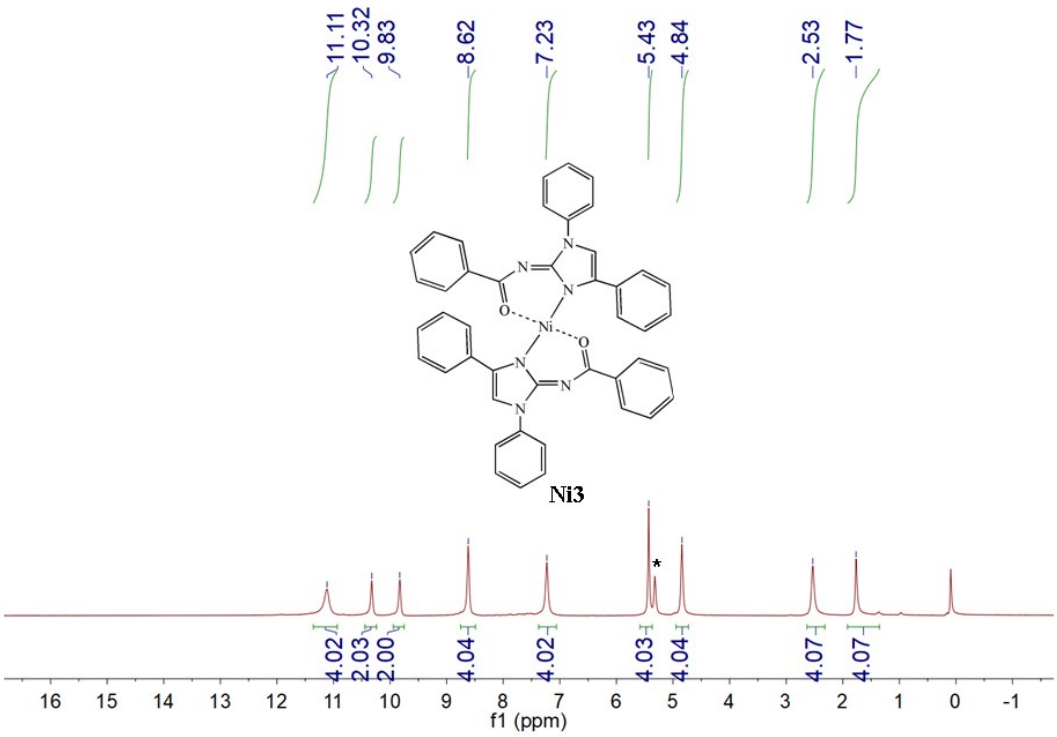

Figure S1-21. ^{1}H NMR spectrum of complex **Ni3** in CD_2Cl_2 (* - CD_2Cl_2)

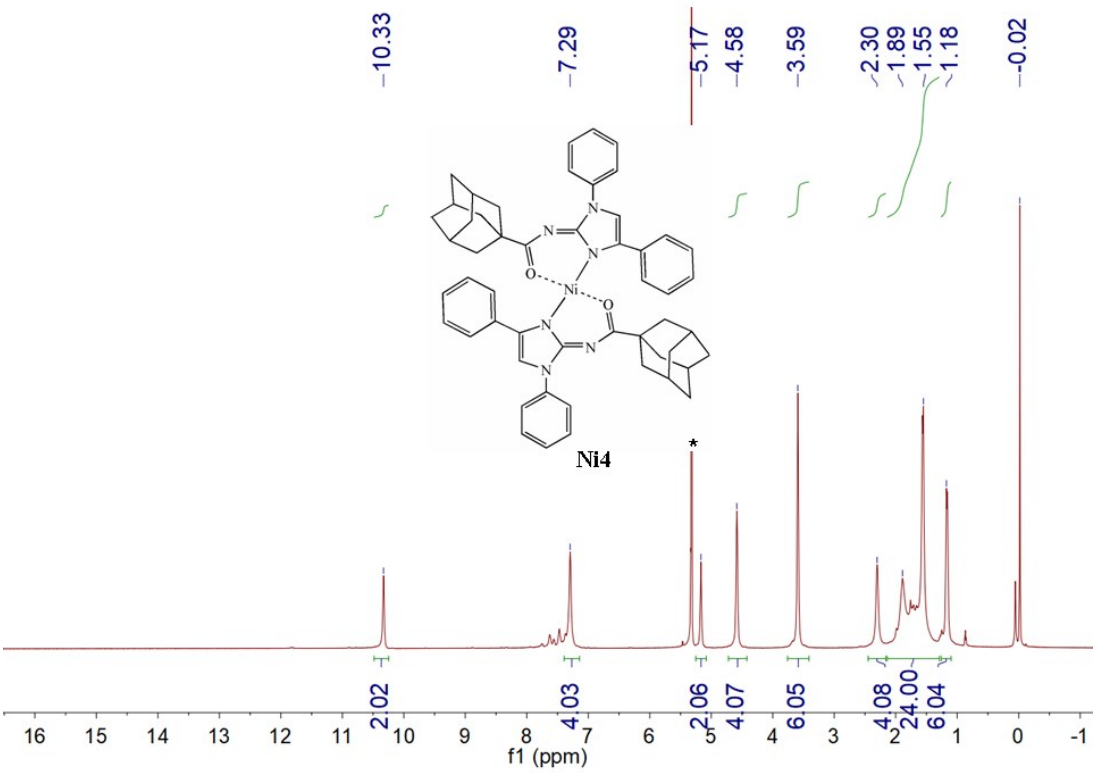

Figure S1-22. ^{1}H NMR spectrum of complex **Ni4** in CD_2Cl_2 (* - CD_2Cl_2)

2. Crystal data and structure refinement for complexes Ni1-Ni4

Table S1. Crystal data and structure refinement for complexes **Ni1-Ni4**

	Ni1	**Ni2**
Empirical formula	$C_{32}H_{24}N_6NiO_2$	$C_{40}H_{44}N_6NiO_2$
Formula weight	583.28	699.52
Temperature (K)	170.01	170.03
Wavelength (Å)	1.34139	1.34139
Crystal system	Triclinic	Triclinic
Space group	P-1	P-1
a (Å)	5.41180(10)	6.3174(2)
b (Å)	15.0266(2)	10.7495(3)
c (Å)	15.9498(3)	12.7292(4)
α (°)	91.1300(10)	74.886(2)
β (°)	96.7910(10)	79.406(2)
γ (°)	92.6390(10)	89.242(2)
Volume ($Å^3$)	1286.17(4)	819.75(4)
Z	2	1
Density (calculated) (Mg/m^3)	1.506	1.417
Absorption coefficient (mm^{-1})	4.438	3.540
F(000)	604	370
Crystal size (mm^3)	0.05×0.015×0.005	0.08×0.01×0.005
Theta range for data collection (°)	4.860 to 54.943	5.491 to 54.961
Index ranges	-6<=h<=6, -18<=k<=18, -17<=l<=19	-7<=h<=7, -12<=k<=13, 0<=l<=15
Reflections collected	15594	3022
Independent reflections	4872 [R(int) = 0.0355]	3022 [R(int) = 0.0580]
Completeness to theta = 26.000°	99.4 %	98.6 %
Absorption correction	Semi-empirical from equivalents	Semi-empirical from equivalents
Max. and min. transmission	0.7508 and 0.6187	0.7508 and 0.5831
Refinement method	Full-matrix least-squares on F^2	Full-matrix least-squares on F^2
Data / restraints / parameters	4872 / 0 / 373	3022 / 0 / 224
Goodness-of-fit on F^2	1.023	1.037
Final R indices [I>2sigma(I)]	R1 = 0.0335, wR2 = 0.0809	R1 = 0.0434, wR2 = 0.1223
R indices (all data)	R1 = 0.0420, wR2 = 0.0859	R1 = 0.0520, wR2 = 0.1374
Extinction coefficient	n/a	n/a
Largest diff. peak and hole ($e.Å^{-3}$)	0.197 and -0.529	0.336 and -0.412

	Ni3	**Ni4**
Empirical formula	$C_{44}H_{32}N_6NiO_2$	$C_{52}H_{52}N_6NiO_2$
Formula weight	735.46	851.70
Temperature (K)	169.98	170.02
Wavelength (Å)	1.34139	1.34139
Crystal system	Monoclinic	Triclinic
Space group	P 1211	P-1
a (Å)	9.8938(18)	11.1027(2)
b (Å)	19.286(3)	12.8123(2)
c (Å)	10.6047(19)	16.5909(3)
α (°)	90	68.3340(10)
β (°)	116.982(13)	89.5930(10)
γ (°)	90	74.9630(10)
Volume ($Å^3$)	1803.2(6)	2107.87(7)
Z	4	2
Density (calculated) (Mg/m^3)	1.355	1.342
Absorption coefficient (mm^{-1})	3.243	2.819
F(000)	764	900
Crystal size (mm^3)	0.05×0.03×0.02	0.12×0.1×0.08
Theta range for data collection (°)	4.070 to 55.468	4.182 to 54.927
Index ranges	-12<=h<=10, -23<=k<=18, -12<=l<=13	-13<=h<=13, -15<=k<=15, -20<=l<=20
Reflections collected	9115	21795
Independent reflections	5790 [R(int) = 0.0800]	7938 [R(int) = 0.0448]
Completeness to theta = 26.000°	99.4 %	98.8 %
Absorption correction	Semi-empirical from equivalents	Semi-empirical from equivalents
Max. and min. transmission	0.7508 and 0.4792	0.7508 and 0.6073
Refinement method	Full-matrix least-squares on F^2	Full-matrix least-squares on F^2
Data / restraints / parameters	5790 / 1 / 479	7938 / 0 / 550
Goodness-of-fit on F^2	0.921	1.068
Final R indices [I>2sigma(I)]	R1 = 0.0666, wR2 = 0.1530	R1 = 0.0367, wR2 = 0.0985
R indices (all data)	R1 = 0.1290, wR2 = 0.1858	R1 = 0.0424, wR2 = 0.1022
Extinction coefficient	n/a	n/a
Largest diff. peak and hole ($e.Å^{-3}$)	0.402 and -0.523	0272 and -0.596

3. NMR spectra, GPC curves and DSC curves of NB-HAc copolymers

3.1. Microstructure of NB-HAc copolymer

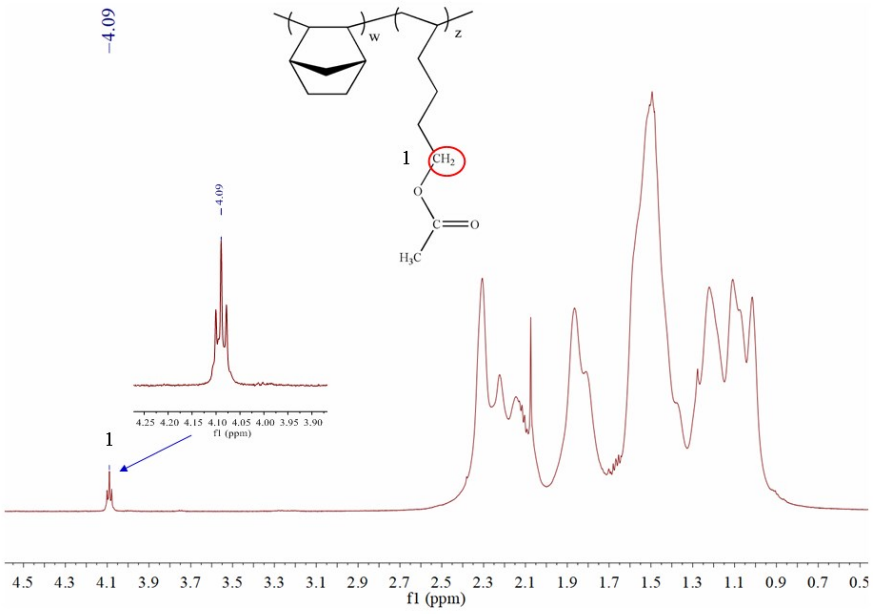

Figure S2-1. [1]H NMR spectra of NB-HAc copolymer obtained by **Ni3** with 30 mol% of HAc (Table 2, entry 6)

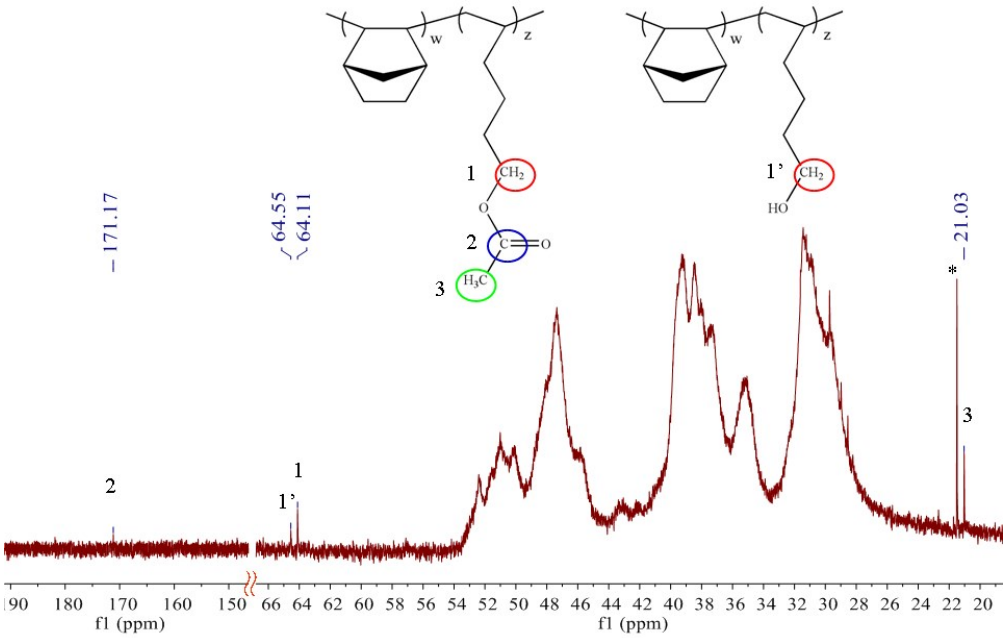

Figure S2-2. [13]C NMR spectra of NB-HAc copolymer obtained by **Ni3** with 30 mol% of HAc (Table 2, entry 6) (*–methyl in toluene).

Around 10 mol% hydroxyl groups were formed by the hydrolysis of the ester groups in the work-up process, which includes a treatment of 10% HCl solution of ethanol.

3.2. HAc incorporation in NB-HAc copolymers obtained by Ni1-Ni4

The incorporation (mol%) of HAc in the copolymer:

$$x = \frac{\frac{I_a}{2}}{\frac{I_a}{2} + \frac{I_b - \frac{I_a}{2} \times 12}{10}} \times 100\% = \frac{5I_a}{I_b - I_a} \times 100\%$$

I_a – The integration of methylene (–CH_2-O-) in HAc units;

I_b – The integration of aliphatic-H in the NB-HAc copolymer.

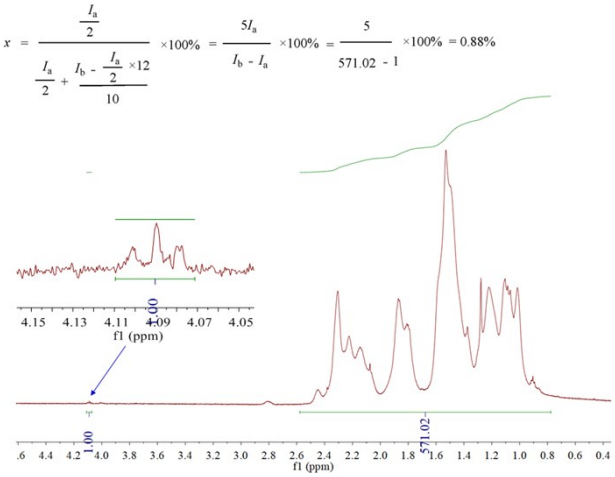

Figure S2-3. HAc incorporation in NB-HAc copolymer obtained by **Ni1** with 5 mol% of HAc (Table 2, entry 1)

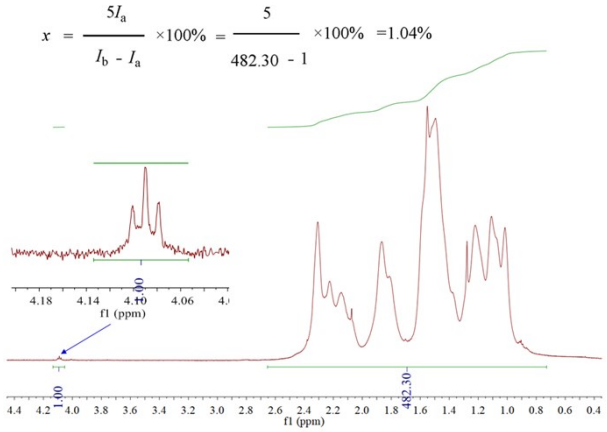

Figure S2-4. HAc incorporation in NB-HAc copolymer obtained by **Ni2** with 10 mol% of HAc (Table 2, entry 2)

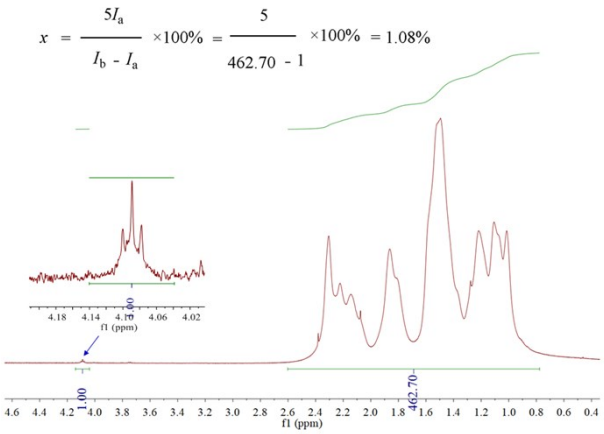

Figure S2-5. HAc incorporation in NB-HAc copolymer obtained by **Ni3** with 10 mol% of HAc (Table 2, entry 3)

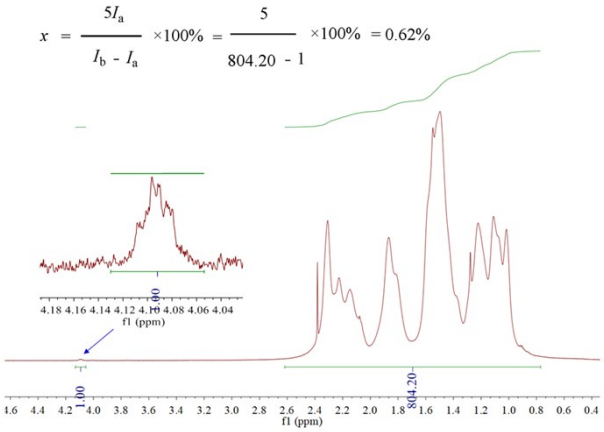

Figure S2-6. HAc incorporation in NB-HAc copolymer obtained by **Ni4** with 10 mol% of HAc (Table 2, entry 4)

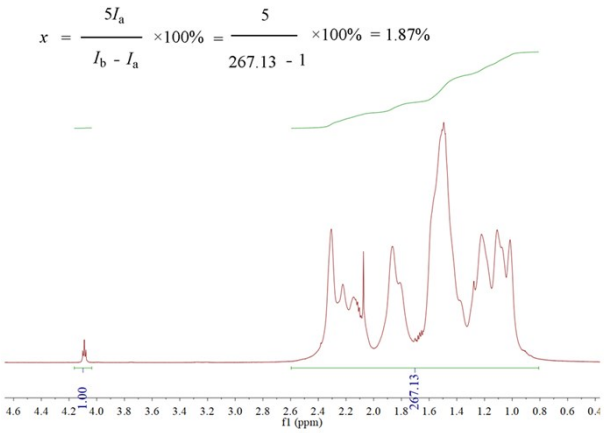

Figure S2-7. HAc incorporation in NB-HAc copolymer obtained by **Ni3** with 20 mol% of HAc (Table 2, entry 5)

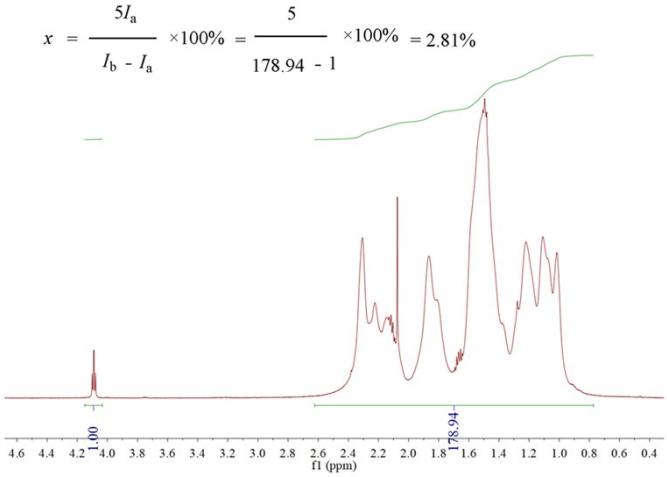

Figure S2-8. HAc incorporation in NB-HAc copolymer obtained by **Ni3** with 30 mol% of HAc (Table 2, entry 6)

4.3. GPC curves of NB-HAc copolymers

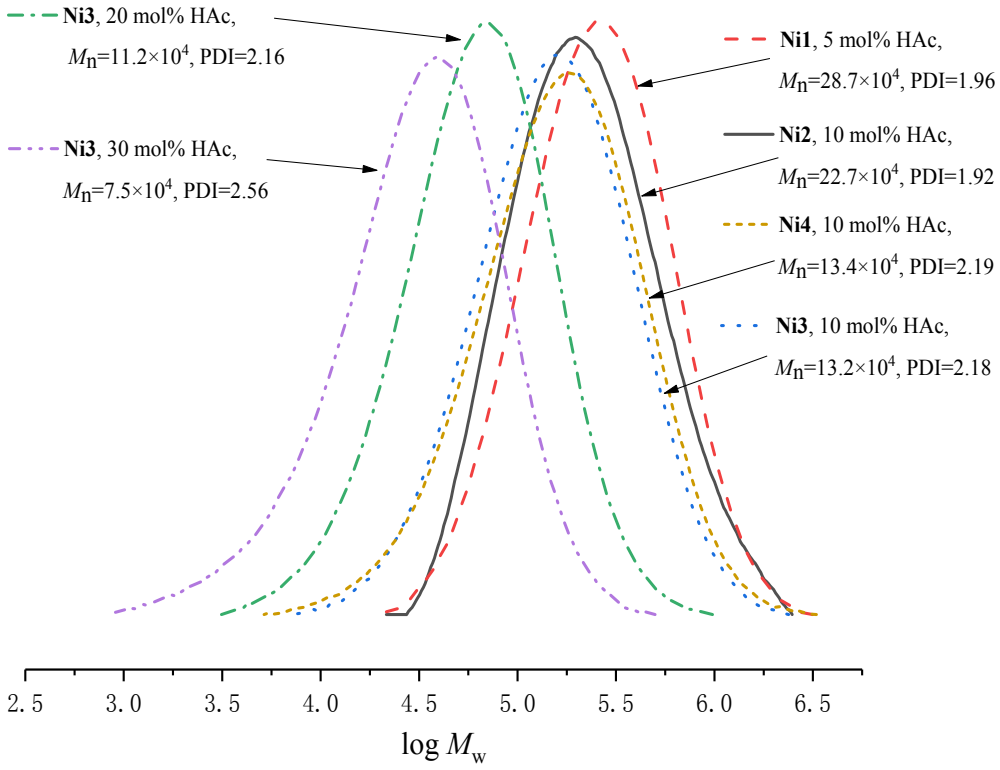

Figure S2-9. GPC curves of NB-HAc copolymers obtained by **Ni1-Ni4**

3.4. DSC curves of NB-HAc copolymers

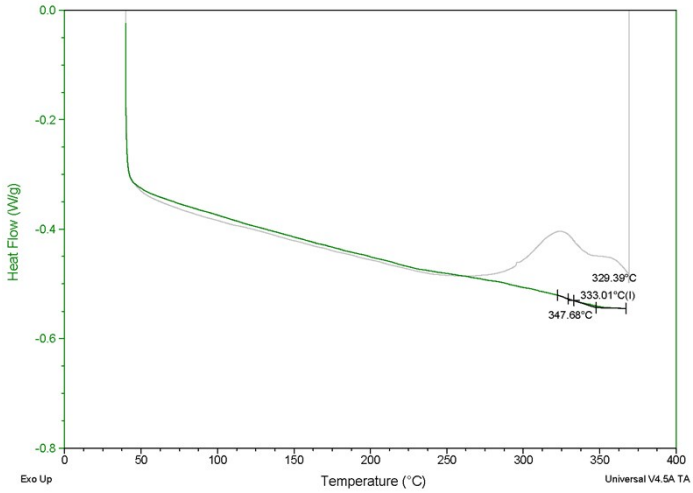

Figure S2-10. DSC curve of NB-HAc copolymer obtained by **Ni1** with 5 mol% of HAc (Table 2, entry 1)

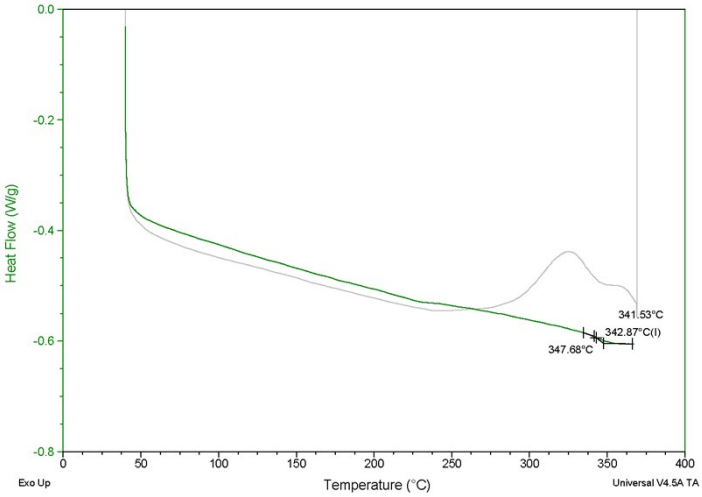

Figure S2-11. DSC curve of NB-HAc copolymer obtained by **Ni2** with 10 mol% of HAc (Table 2, entry 2)

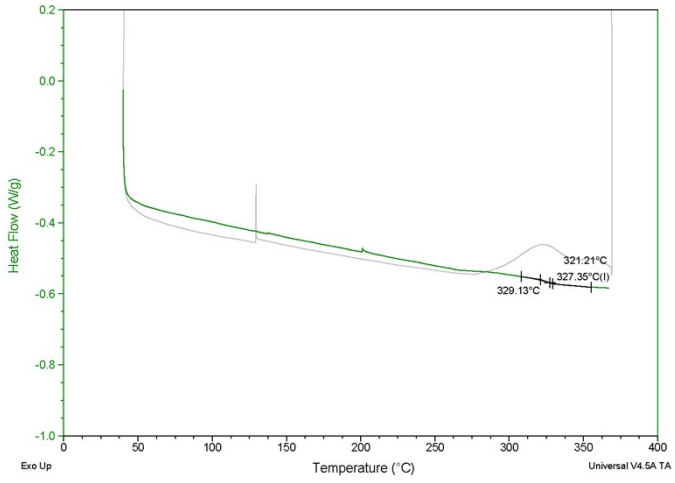

Figure S2-12. DSC curve of NB-HAc copolymer obtained by **Ni3** with 10 mol% of HAc (Table 2, entry 3)

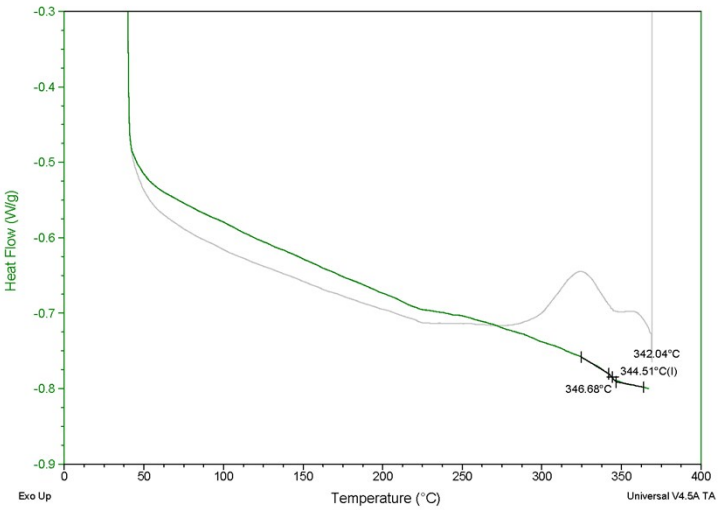

Figure S2-13. DSC curve of NB-HAc copolymer obtained by **Ni4** with 10 mol% of HAc (Table 2, entry 4)

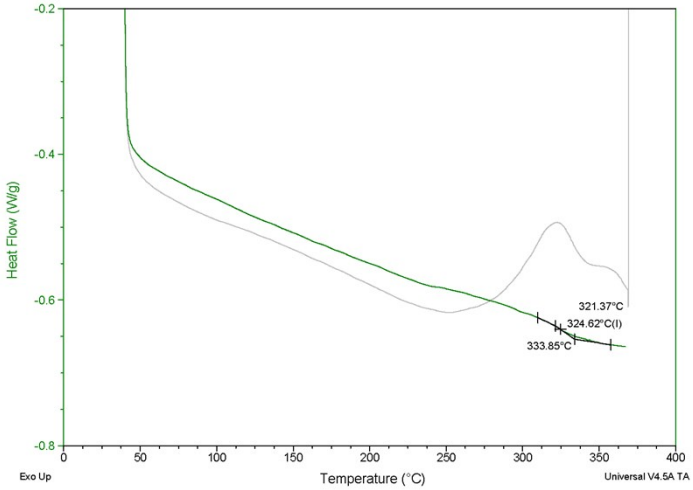

Figure S2-14. DSC curve of NB-HAc copolymer obtained by **Ni3** with 20 mol% of HAc (Table 2, entry 5)

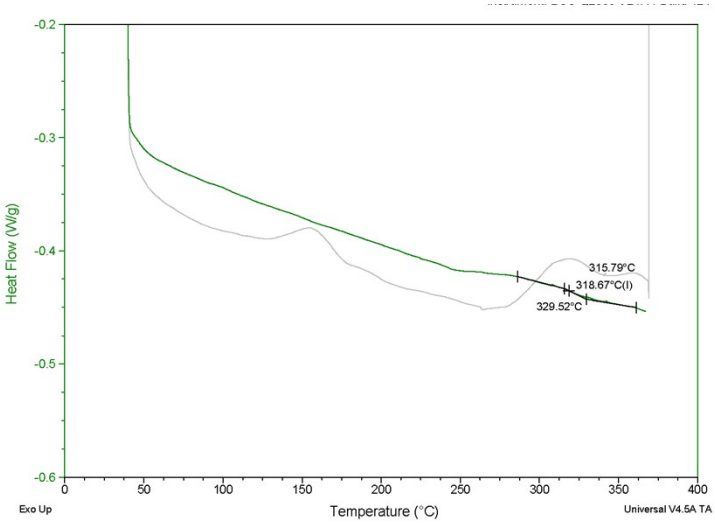

Figure S2-15. DSC curve of NB-HAc copolymer obtained by **Ni3** with 30 mol% of HAc (Table 2, entry 6)

4. NMR spectra, GPC curves and DSC curves of NB-AAc copolymers

4.1. Microstructure of NB-AAc copolymer

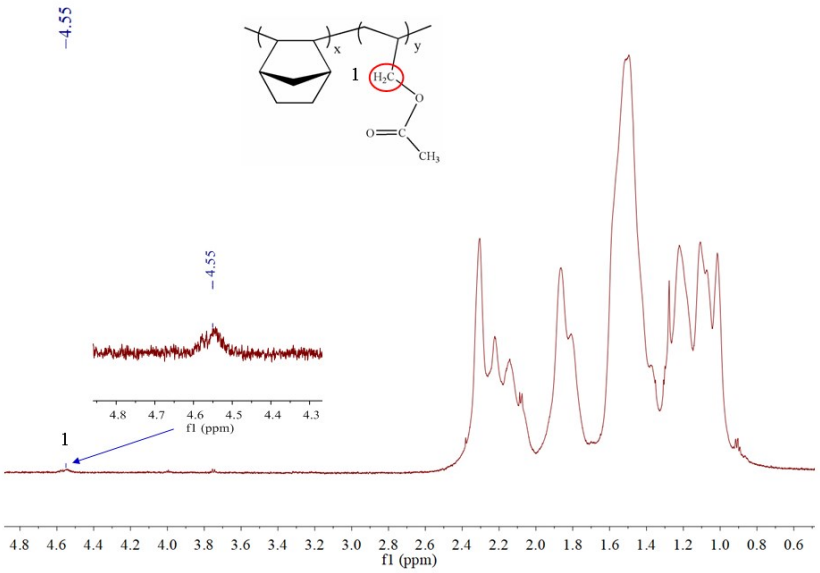

Figure S3-1. [1]H NMR spectra of NB-AAc copolymer obtained by **Ni3** with 20 mol% of AAc (Table 2, entry 12)

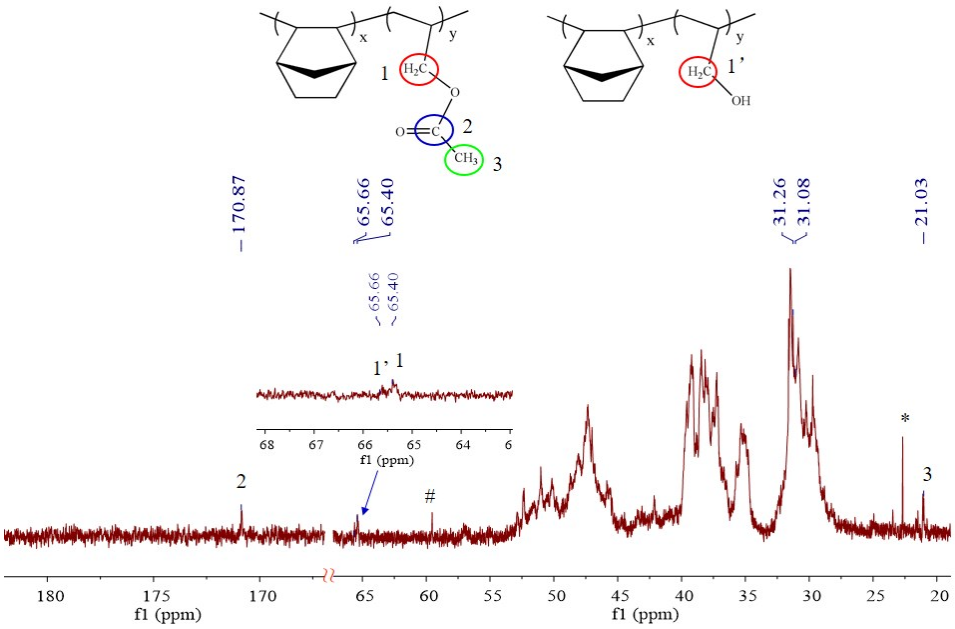

Figure S3-2. [13]C NMR spectra of NB-AAc copolymer obtained by **Ni3** with 20 mol% of AAc (Table 2, entry 12) (* – methyl in toluene; # – methylene in ethanol).
The hydroxyl groups were formed by the hydrolysis of the ester groups in the work-up process, which includes a treatment of 10% HCl solution of ethanol.

4.2. AAc incorporation in NB-AAc copolymers obtained by Ni1-Ni4

The incorporation (mol%) of AAc in the copolymer:

$$x = \frac{\frac{I_a}{2}}{\frac{I_a}{2} + \frac{I_b - \frac{I_a}{2} \times 6}{10}} \times 100\% = \frac{5I_a}{I_b + 2I_a} \times 100\%$$

I_a – The integration of methylene (–CH_2-O-) in AAc units;

I_b – The integration of aliphatic-H in the NB-AAc copolymer.

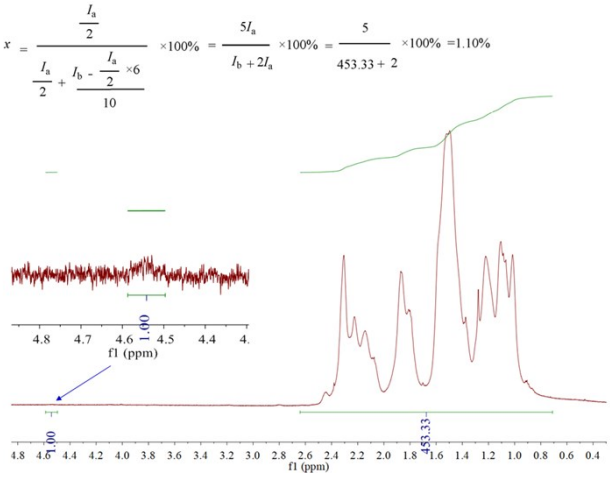

Figure S3-3. AAc incorporation in NB-AAc copolymer obtained by **Ni1** with 5 mol% of AAc (Table 2, entry 8)

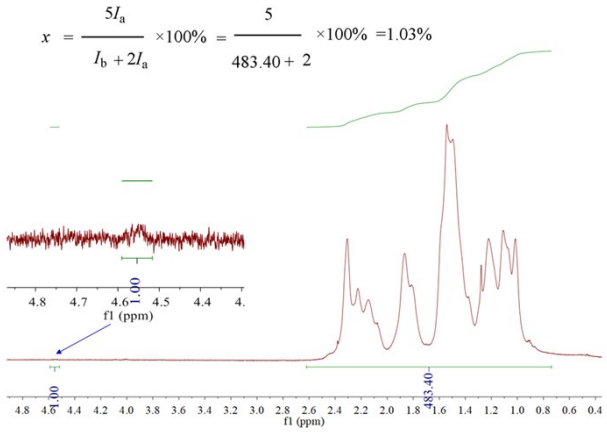

Figure S3-4. AAc incorporation in NB-AAc copolymer obtained by **Ni2** with 5 mol% of AAc (Table 2, entry 9)

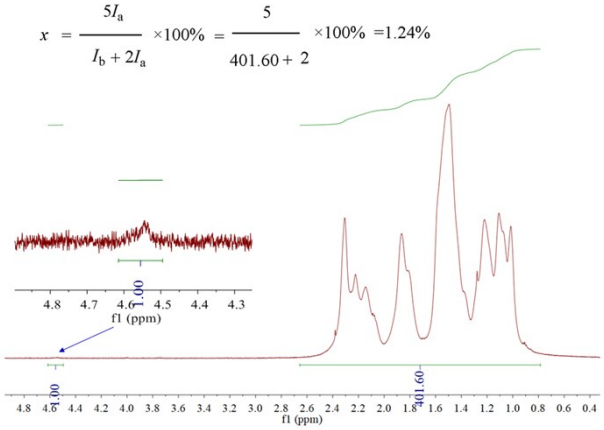

Figure S3-5. AAc incorporation in NB-AAc copolymer obtained by **Ni3** with 5 mol% of AAc (Table 2, entry 10)

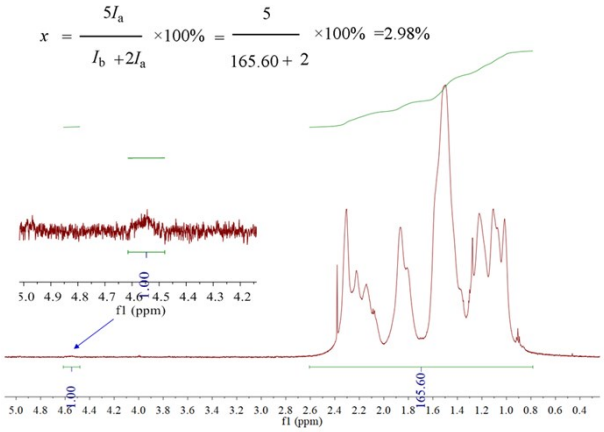

Figure S3-6. AAc incorporation in NB-AAc copolymer obtained by **Ni3** with 10 mol% of AAc (Table 2, entry 11)

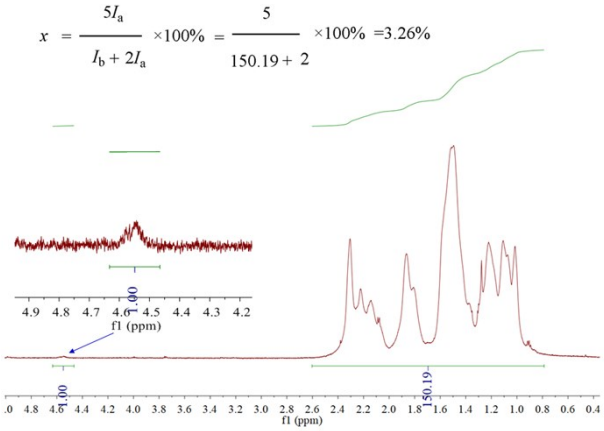

Figure S3-7. AAc incorporation in NB-AAc copolymer obtained by **Ni3** with 20 mol% of AAc (Table 2, entry 12)

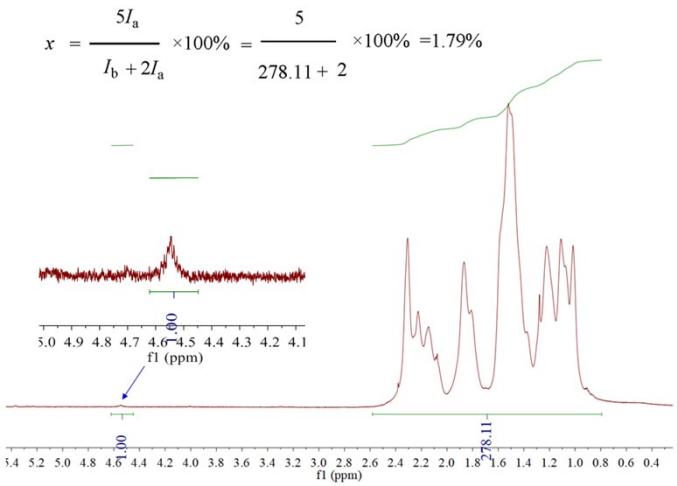

Figure S3-8. AAc incorporation in NB-AAc copolymer obtained by **Ni4** with 42 mol% of AAc (Table 2, entry 13)

4.3. GPC curves of NB-AAc copolymers

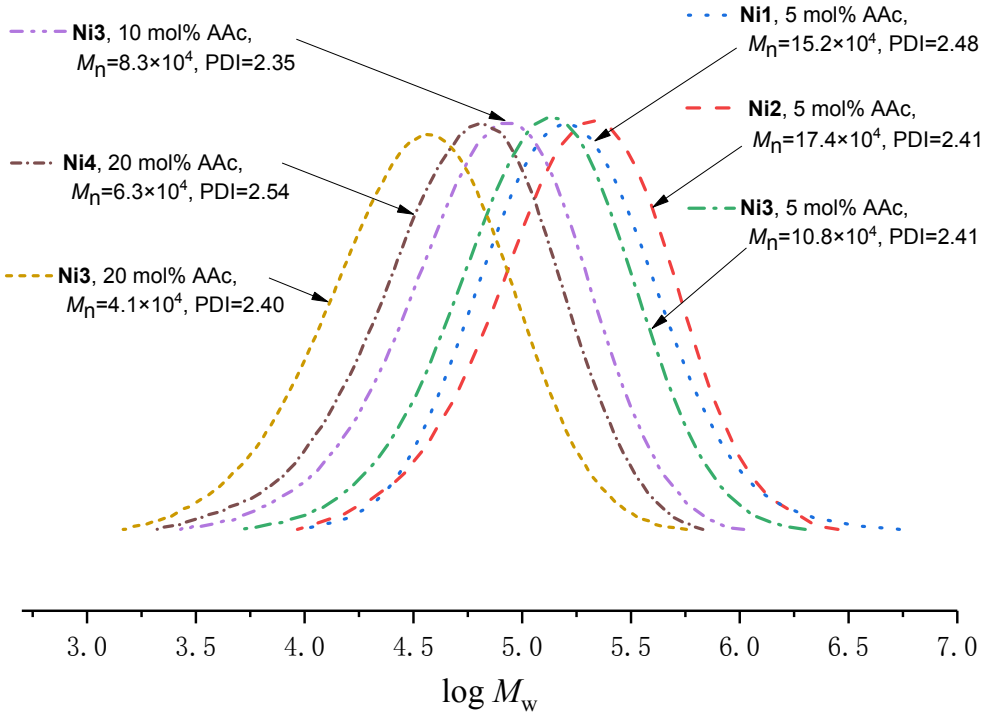

Figure S3-9. GPC curves of NB-AAc copolymers obtained by **Ni1**-**Ni4**

4.4. DSC curves of NB-AAc copolymers

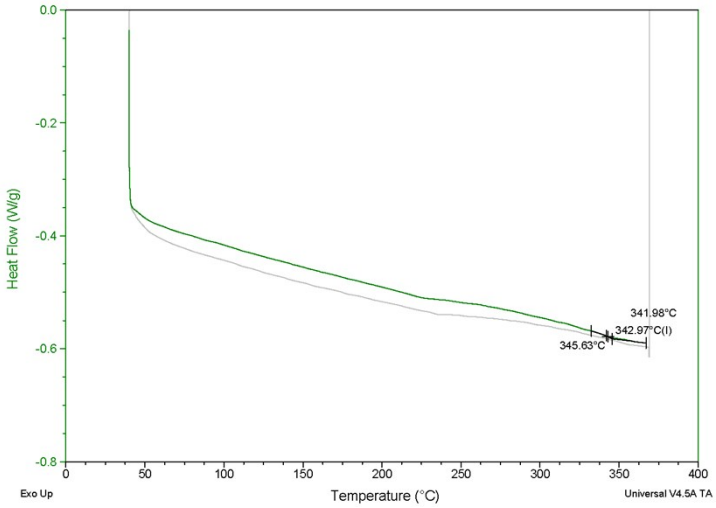

Figure S3-10. DSC curve of NB-AAc copolymer obtained by **Ni** with 5 mol% of AAc (Table 2, entry 8)

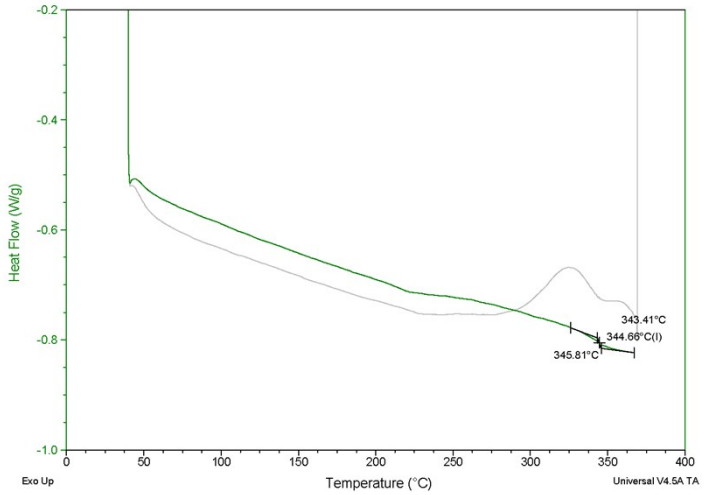

Figure S3-11. DSC curve of NB-AAc copolymer obtained by **Ni2** with 5 mol% of AAc (Table 2, entry 9)

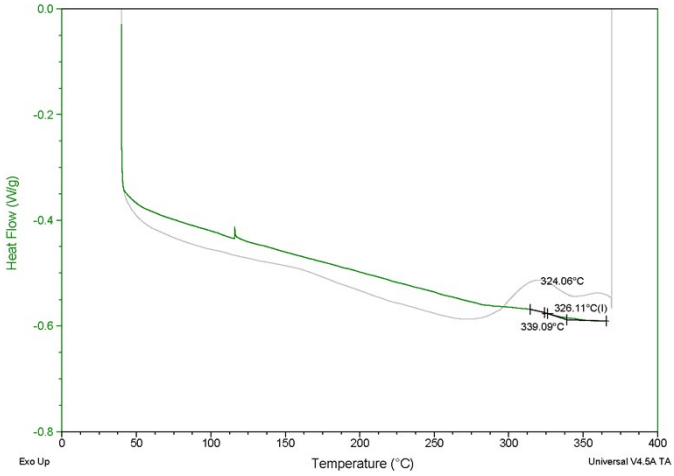

Figure S3-12. DSC curve of NB-AAc copolymer obtained by **Ni3** with 5 mol% of AAc (Table 2, entry 10)

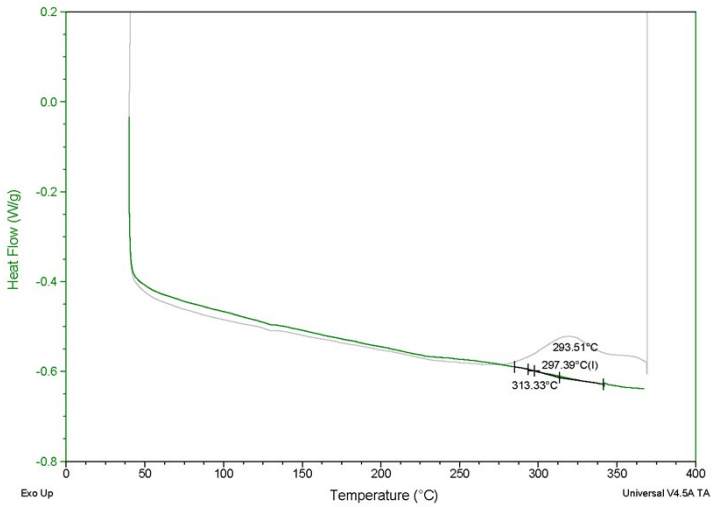

Figure S3-13. DSC curve of NB-AAc copolymer obtained by **Ni3** with 10 mol% of AAc (Table 2, entry 11)

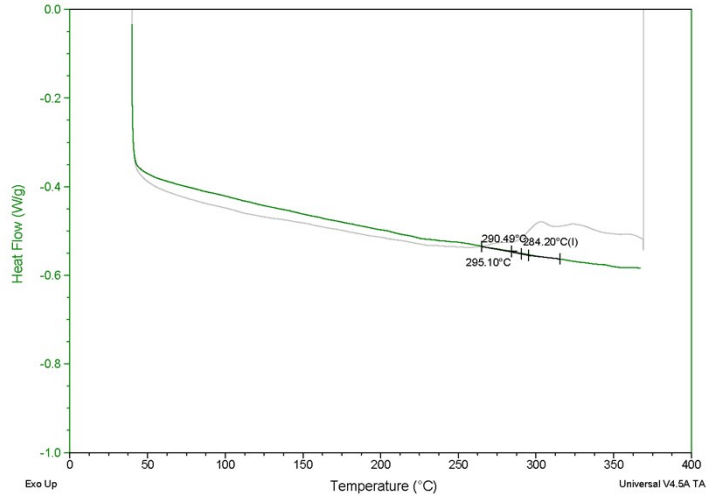

Figure S3-14. DSC curve of NB-AAc copolymer obtained by **Ni3** with 20 mol% of AAc (Table 2, entry 12)

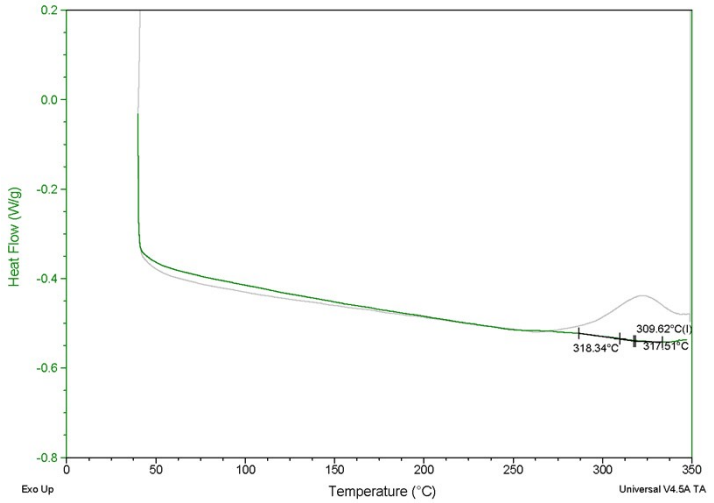

Figure S3-15. DSC curve of NB-AAc copolymer obtained by **Ni4** with 20 mol% of AAc (Table 2, entry 13)

5. NMR spectra, GPC curves and DSC curves of NB-MA copolymers

5.1. Microstructure of NB-MA copolymer

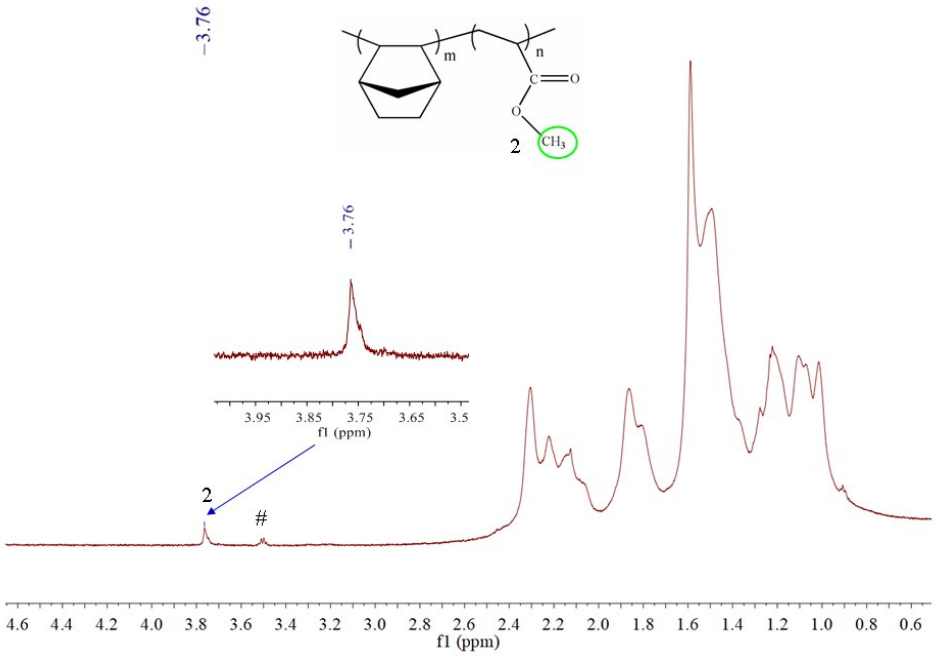

Figure S4-1. [1]H NMR spectra of NB-MA copolymer obtained by **Ni3** with 10 mol% of MA (Table 2, entry 18) (# – methylene in ethanol)

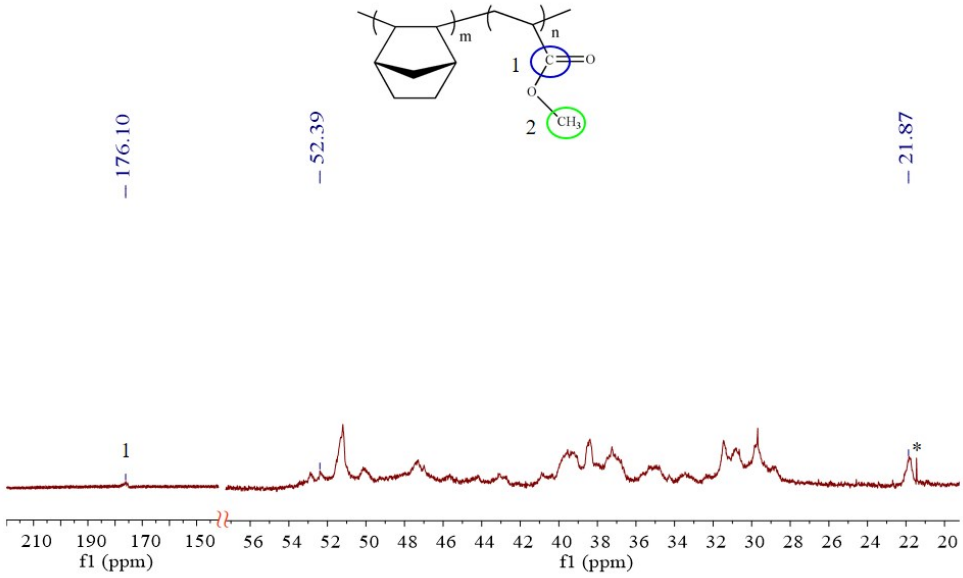

Figure S4-2. [13]C NMR spectra of NB-MA copolymer obtained by **Ni3** with 10 mol% of MA (Table 2, entry 18) (* – methyl in toluene)

5.2. MA incorporation in NB-MA copolymers obtained by Ni1-Ni4

The incorporation (mol%) of MA in the copolymer:

$$x = \frac{\frac{I_a}{3}}{\frac{I_a}{3} + \frac{I_b - \frac{I_a}{3} \times 3}{10}} \times 100\% = \frac{10I_a}{3I_b + 7I_a} \times 100\%$$

I_a – The integration of methyl group (-OCH_3) in MA units;

I_b – The integration of aliphatic-H in the NB-MA copolymer.

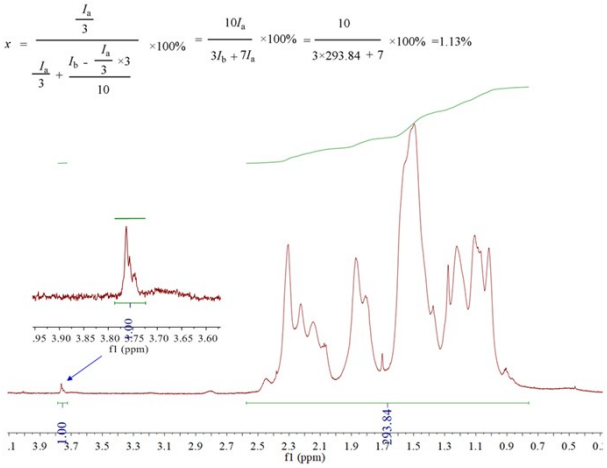

Figure S4-3. MA incorporation in NB-MA copolymer obtained by **Ni1** with 5 mol% of MA (Table 2, entry 15)

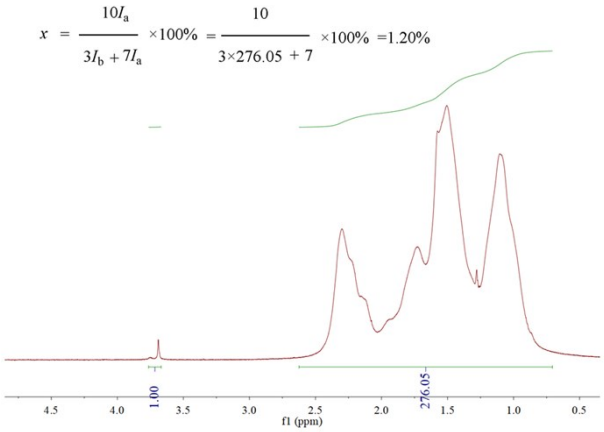

Figure S4-4. MA incorporation in NB-MA copolymer obtained by **Ni2** with 5 mol% of MA (Table 2, entry 16)

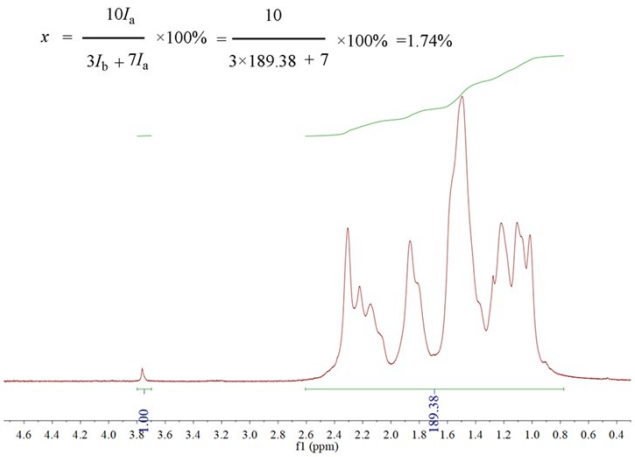

Figure S4-5. MA incorporation in NB-MA copolymer obtained by **Ni3** with 5 mol% of MA (Table 2, entry 17)

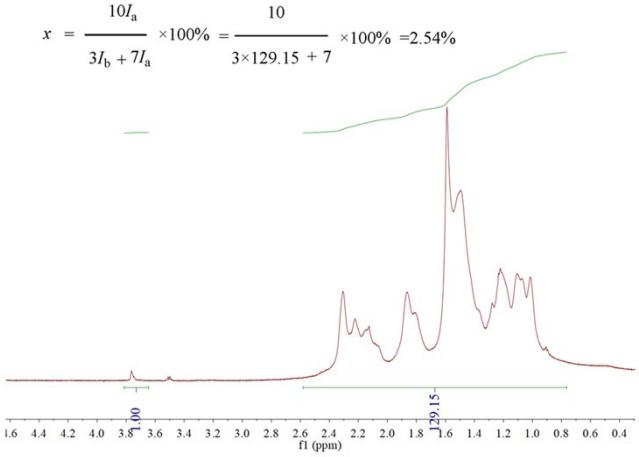

Figure S4-6. MA incorporation in NB-MA copolymer obtained by **Ni3** with 10 mol% of MA (Table 2, entry 18)

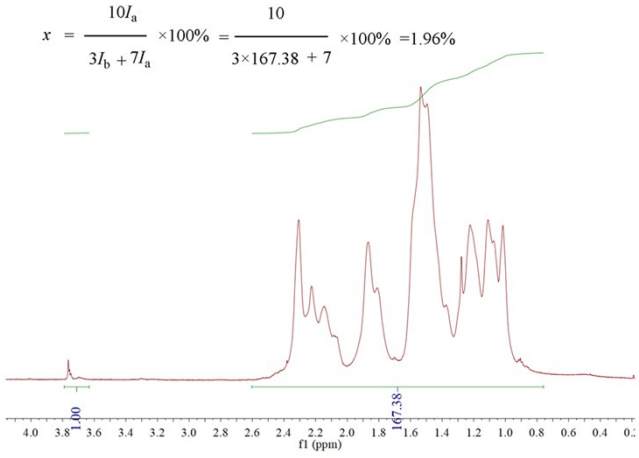

Figure S4-7. MA incorporation in NB-MA copolymer obtained by **Ni4** with 10 mol% of MA (Table 2, entry 19)

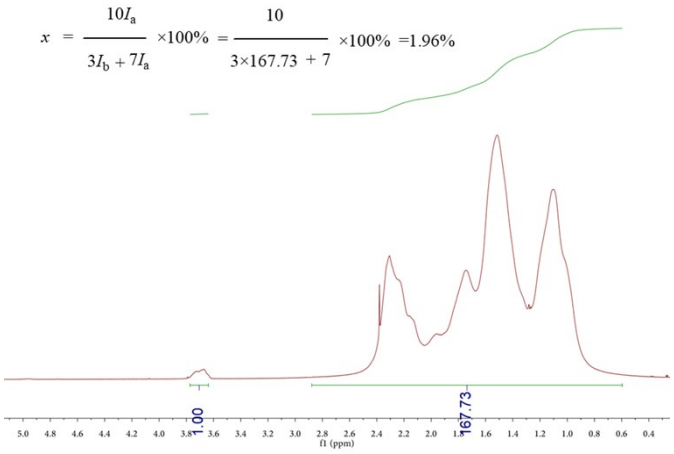

Figure S4-8. MA incorporation in NB-MA copolymer obtained by **Ni3** with 5 mol% of MA (60 ℃, Table 2, entry 21)

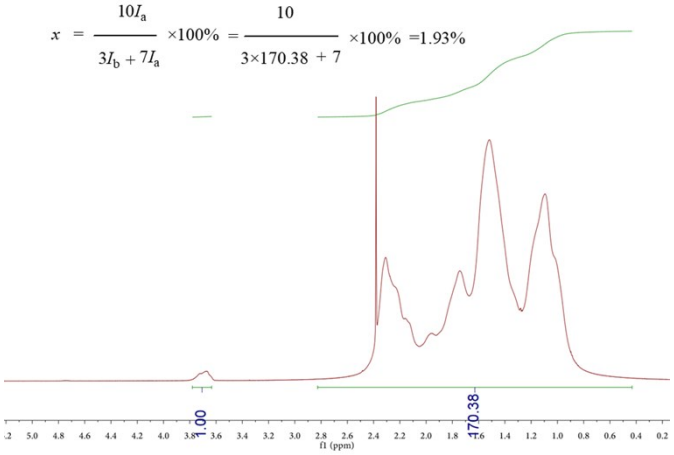

Figure S4-9. MA incorporation in NB-MA copolymer obtained by **Ni3** with 5 mol% of MA (80 ℃, Table 2, entry 22)

5.3. GPC curves of NB-MA copolymers

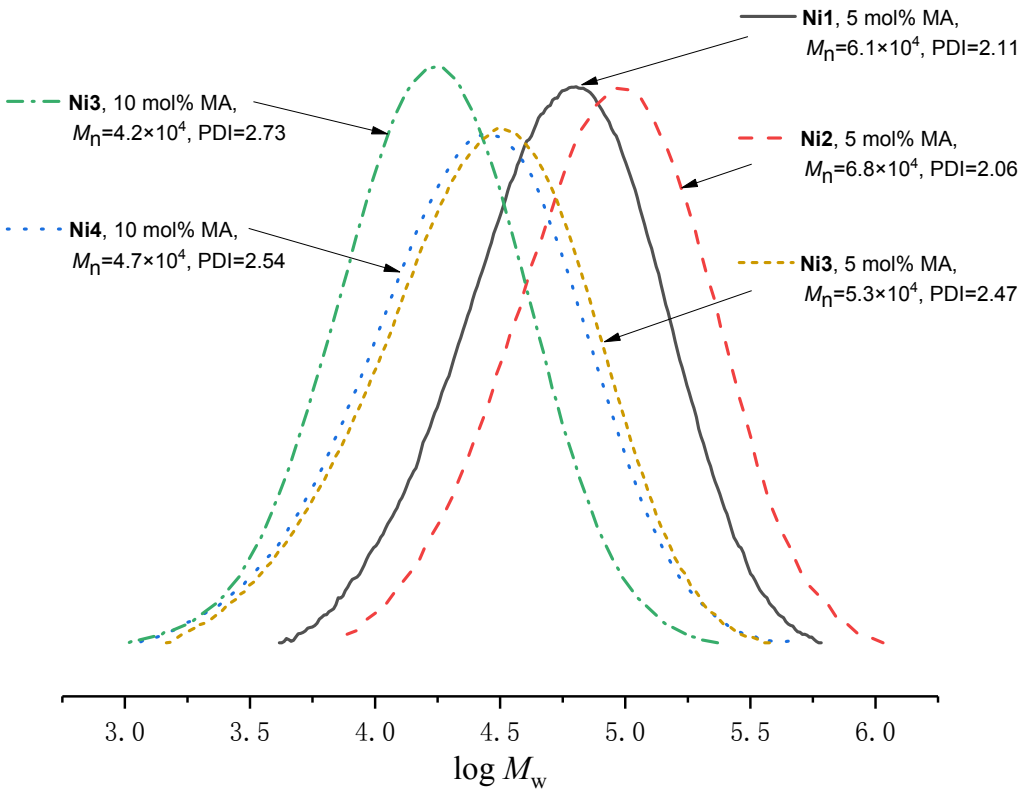

Figure S4-10. GPC curves of NB-MA copolymers obtained by **Ni1**-**Ni4**

5.4. DSC curves of NB-MA copolymers

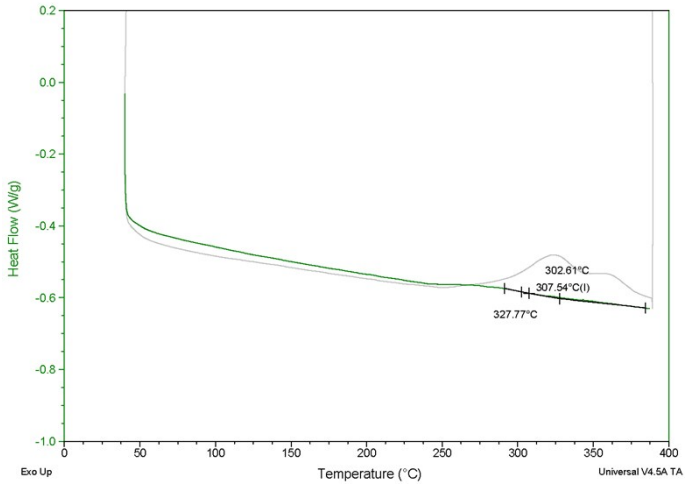

Figure S4-11. DSC curve of NB-MA copolymer obtained by **Ni1** with 5 mol% of MA (Table 2, entry 15)

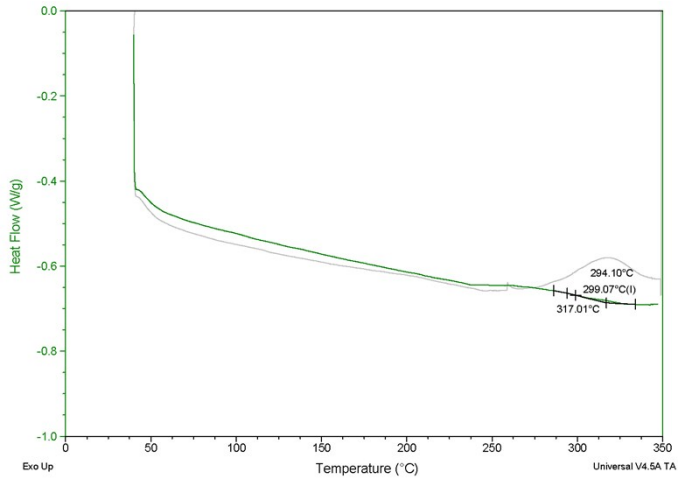

Figure S4-12. DSC curve of NB-MA copolymer obtained by **Ni2** with 5 mol% of MA (Table 2, entry 16)

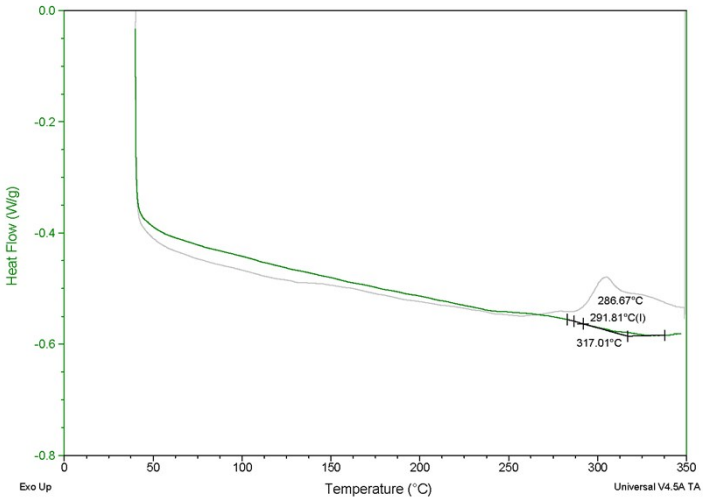

Figure S4-13. DSC curve of NB-MA copolymer obtained by **Ni3** with 5 mol% of MA (Table 2, entry 17)

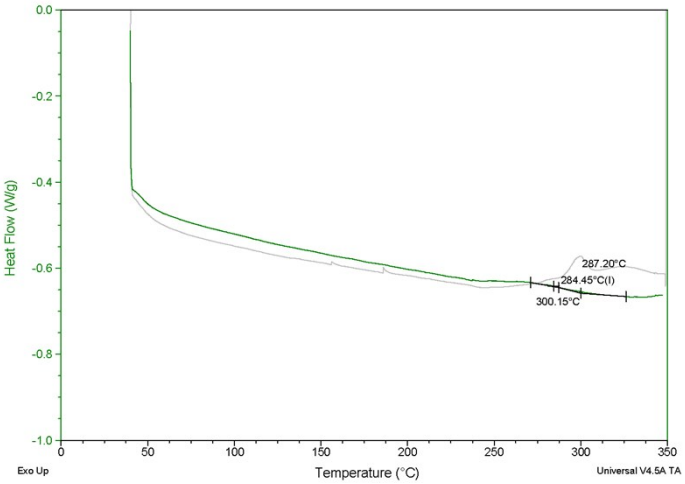

Figure S4-14. DSC curve of NB-MA copolymer obtained by **Ni3** with 10 mol% of MA (Table 2, entry 18)

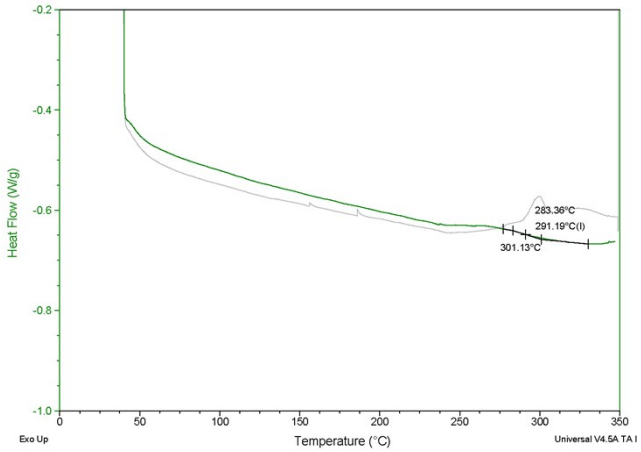

Figure S4-15. DSC curve of NB-MA copolymer obtained by **Ni4** with 10 mol% of MA (Table 2, entry 19)